Epidemics 21 (2017) 63–79

Contents lists available at ScienceDirect

Epidemics

journal homepage: www.elsevier.com/locate/epidemics

Estimating the reproductive number, total outbreak size, and reporting rates for Zika epidemics in South and Central America

Deborah P. Shutt[a,*], Carrie A. Manore[c,d,e], Stephen Pankavich[b], Aaron T. Porter[b], Sara Y. Del Valle[d]

[a] Department of Applied Mathematics, Virginia Military Institute, Lexington, VA 24450, United States
[b] Department of Applied Mathematics and Statistics, Colorado School of Mines, Golden, CO 80401, United States
[c] Theoretical Biology and Biophysics, Los Alamos National Laboratory, Los Alamos, NM 87544, United States
[d] Information Systems and Modeling, Los Alamos National Laboratory, Los Alamos, NM 87544, United States
[e] The New Mexico Consortium, Los Alamos, NM 87544, United States

ARTICLE INFO

Article history:
Received 17 February 2017
Received in revised form 14 June 2017
Accepted 27 June 2017
Available online 13 July 2017

ABSTRACT

As South and Central American countries prepare for increased birth defects from Zika virus outbreaks and plan for mitigation strategies to minimize ongoing and future outbreaks, understanding important characteristics of Zika outbreaks and how they vary across regions is a challenging and important problem. We developed a mathematical model for the 2015/2016 Zika virus outbreak dynamics in Colombia, El Salvador, and Suriname. We fit the model to publicly available data provided by the Pan American Health Organization, using Approximate Bayesian Computation to estimate parameter distributions and provide uncertainty quantification. The model indicated that a country-level analysis was not appropriate for Colombia. We then estimated the basic reproduction number to range between 4 and 6 for El Salvador and Suriname with a median of 4.3 and 5.3, respectively. We estimated the reporting rate to be around 16% in El Salvador and 18% in Suriname with estimated total outbreak sizes of 73,395 and 21,647 people, respectively. The uncertainty in parameter estimates highlights a need for research and data collection that will better constrain parameter ranges.

1. Introduction

Mosquito-borne diseases contribute significantly to the overall morbidity and mortality caused by infectious diseases in Central and South America. Newly emergent pathogens, such as Zika virus in 2015, highlight the need for data and models to understand the public health impact of associated diseases and develop mitigation strategies to combat their spread. In particular, since Zika virus is a newly emergent pathogen in the Americas, its impact on the naïve population is relatively unknown.

The disease was first discovered in isolation from a rhesus macaque in the Zika forest of Uganda in 1974 (World Health Organization, 2017a,b). While infrequent human cases were confirmed in later years in both Africa and Southeast Asia, it was not until April 2007 that an outbreak outside of these traditional areas occurred on Yap Island in the North Pacific (Duffy et al., 2009), and this was followed by another outbreak occurring in French Polynesia beginning October of 2013 (Kucharski et al., 2016). However, the most significant Zika outbreak began within Central and South America in 2015 (World Health Organization, 2016) and is currently ongoing. Thus far it has resulted in an estimated 781,914 cases, which includes both suspected and confirmed cases within Latin American and Non-Latin Caribbean countries (accessed August 1, 2017) (Pan American Health Organization, 2017). This study focuses on the behavior of the recent epidemics in Colombia, El Salvador, and Suriname.

Zika is transmitted to humans primarily through bites from infected *Aedes aegypti* and *Aedes albopictus* mosquitoes. The transmission is in both directions, that is, infected mosquitoes infect humans and infected humans infect mosquitoes. Upon transmission of the virus from mosquito to human, an individual will become infectious within 3–12 days. Symptoms of infection include fever, rash, joint pain, conjunctivitis, muscle pain and headache. Recovery from Zika virus disease may require anywhere from 3 to 14 days after becoming infectious, but once recovered humans are believed to be immune from the virus for life (Dudley et al., 2016; Hyer and Covello, 2017; World Health Organization, 2017a,b). Many people infected with Zika may be asymptomatic or will only

* Corresponding author.
E-mail address: shuttda@vmi.edu (D.P. Shutt).

http://dx.doi.org/10.1016/j.epidem.2017.06.005

display mild symptoms that do not require medical attention. An estimated 80% of persons infected with Zika virus are asymptomatic (Petersen et al., 2016; Duffy et al., 2009; Center for Disease Control, 2016a,b). Thus, there is a high occurrence of under-reporting for Zika cases. In fact, the number of infected individuals who report their symptoms is estimated to be between 7% and 17% (Kucharski et al., 2016) of the total number infected by the virus.

Zika can also be transmitted vertically, as a mother can pass the virus to her child during pregnancy, and this can lead to a variety of developmental issues for the child. Most notably, Zika is a cause of microcephaly and other severe fetal brain defects (Center for Disease Control, 2016a,b). The potential for sexual transmission of Zika virus has also been confirmed (Ortenzio et al., 2016). For instance, the Center for Disease Control (CDC) has determined that Zika can remain in semen longer than in other body fluids, including vaginal fluids, urine, and blood. It should be noted, however, that while these latter means of transmission exist, the number of new human infections produced in this way is relatively low compared to mosquito-borne infections (Cauchemez et al., 2016; Towers et al., 2016; Gao et al., 2016; Coelho et al., 2016), and therefore, in the interest of simplicity and reducing the number of parameters to fit, we will neglect them in formulating a model.

In general, mathematical modeling has been extensively used to understand disease dynamics and the impact of mitigation strategies (Hethcote, 2000). A few recent papers have developed models that focus on the behavior of the Zika epidemic. For example, Gao et al. (2016), proposed an SEIR/SEI model to understand the effects of sexually transmitted Zika in Brazil, Colombia, and El Salvador. However, the authors did not distinguish between countries as they assumed that the three nations of interest share common parameter values. Additionally, Towers et al. (2016) presented a model that incorporates spatial heterogeneity in populations at the city level. Their model focused specifically on the spread of Zika within Barranquilla, Colombia and included a sexual transmission term, but concluded that the effects are not significant enough to sustain the disease in the absence of mosquitoes. A point estimate of the basic reproductive number was obtained using maximum likelihood methods. Other cities in Colombia, San Andres and Girardot, were examined by Rojas et al. (2016) to estimate the reproductive number using likelihood methods to fit a chain binomial model to daily incidence data. The authors assumed the reporting rate to be known and constant at 10%. A study of the impact of short term dispersal on the dynamics of Zika virus is analyzed in Moreno et al. (2016). The model formulated within Moreno et al. (2016) does distinguish between asymptomatic and symptomatic infected populations, and focuses on the estimation of the reproductive number between two close communities. A few studies have modeled Zika in other regions of South America, including Salvador and Rio de Janeiro, Brazil (Cardoso et al., 2015; Villela et al., 2017).

In contrast to previous studies, we adopt an approach to understanding the dynamics of the current Zika epidemic at the country level and present a model that can be used to study disease transmission particular to each country of interest. We identify differences between countries in regards to parameter values and reproductive numbers. We discuss the appropriateness of country level analysis for Colombia, El Salvador, and Suriname and quantify the uncertainty within the resulting biological parameter values.

In the following section, we develop a Susceptible-Exposed-Infectious-Recovered (SEIR) type model which distinguishes between the reported infected population, who are considered symptomatic, and the unreported infected population, who may be asymptomatic or experience symptoms that are not severe enough to seek medical attention. The data available from the Pan American Health Organization (PAHO) serves to motivate the use of a split infectious population. The number of reported cases of Zika, both suspected and confirmed, is reported from PAHO by country.

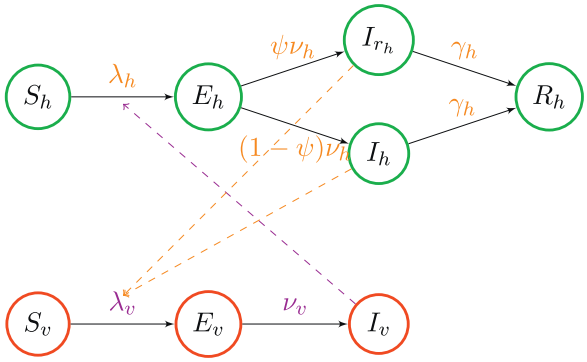

Fig. 1. A schematic representation of (1), modeling the progression of Zika in human populations, denoted by green circles, and mosquito populations, represented with red circles. Susceptible humans start in S_h, and move to E_h, the exposed population, once infected by a mosquito carrying the virus. After an intrinsic incubation period, exposed individuals become infectious and transition to either the reported infectious population, I_{r_h}, or the unreported infectious population, I_r. Infectious humans will then move to and remain in R_h after recovering from the infection. The susceptible mosquito population is denoted S_v. After transmission occurs from bitting an infectious human, susceptible mosquitoes transition to the exposed population, E_v. The end of the extrinsic incubation period marks the exposed mosquitoes shift to the infectious class I_v, where they remain infectious until death.

Hence, we develop a model for three countries of interest assuming that the dynamics of the disease within each may be associated with different parameter values. In Section 3, we address the additional complication that the total population of a country cannot be used as the initial susceptible population due to the biology and bionomics of the *Aedes* species and human contact with them, varying in regards to temperature, humidity (Fay, 1964), sanitation, demographics and elevation (Lozano-Fuentes et al., 2012). Not everyone within a country is equally susceptible to the Zika infection due to geographic diversity; hence, we calculate the unique at-risk population within each country to use as the initial susceptible population. Using the deterministic model at baseline parameter values, the at-risk population we compute yields realistic initial conditions that compare well with PAHO data. With the initial population sizes for the epidemic in each country known and fixed, we embed the deterministic system into a stochastic process to quantify the uncertainty of the parameter values. This method allows us to use biologically valid parameter ranges and Approximate Bayesian Computation (ABC) methods to obtain parameter distributions that are distinct to each country. Section 4 provides a detailed explanation of our implementation of the ABC method along with the strengths and weaknesses discovered in applying this method to our particular model. We summarize the results of the obtained posterior distributions in Section 5. The last section is dedicated to discussion and conclusions.

2. A deterministic Zika model: vector-borne SEIR with case reporting

The spread of Zika relies primarily on interactions between humans and mosquitoes. In this model, we assumed homogeneous mixing between the mosquito and the at-risk human populations as well as uniform susceptibility and infectivity. The parameters are assumed to be time and space invariant. These assumptions are similar to other published models for mosquito-borne disease (Kucharski et al., 2016; Manore et al., 2014). In Fig. 1, members of the at-risk human population, S_h, are bitten by an infectious mosquito and become exposed, or infected without yet being infectious, at a rate λ_h. Humans within the exposed population, E_h, progress from this state to the infectious compartment at a per capita rate, ν_h. Note that there is a portion of infectious humans who are either asymptomatic or experience less severe symptoms,

Table 1
Description of human and mosquito populations state variables.

S_h	Number of susceptible humans
E_h	Number of infected humans who are not yet infectious
I_{r_h}	Number of reported infectious humans
I_h	Number of unreported infectious humans
R_h	Number of recovered humans
S_v	Number of susceptible mosquitoes
E_v	Number of infected mosquitoes who are not yet infectious
I_v	Number of infectious mosquitoes

and therefore go unreported. The parameter ψ denotes the proportion of humans who seek medical assistance and are reported as either suspected or confirmed Zika patients. Thus, there are two categories for infectious humans: I_{r_h}, the reported infectious population, and I_h, the unreported infectious population. Both infectious populations then recover at the same per capita rate of γ_h, where $\frac{1}{\gamma_h}$ is the average time spent as infectious. Upon recovery, we assume humans acquire lifetime immunity. Similarly, a member of the susceptible mosquito population, S_v, becomes exposed at a rate λ_v when susceptible mosquitoes bite an infectious human, resulting in transmission. The exposed mosquitoes, E_v, transition to the infectious compartment at a per capita rate ν_v, where $\frac{1}{\nu_v}$ is the average extrinsic incubation period. Once a mosquito is infectious it will remain so for the duration of its lifespan which can range between 8 and 35 days (Andraud et al., 2012; Otero et al., 2006; Fay, 1964). Finally, because of the long duration of infection for mosquitoes relative to their lifespan, demography (i.e., births and deaths) is included within their population dynamics. In total, the system is described by the following eight coupled, nonlinear ordinary differential equations:

$$\left.\begin{aligned}
\frac{dS_h}{dt} &= -\lambda_h(t)S_h \\
\frac{dE_h}{dt} &= \lambda_h(t)S_h - \nu_h E_h \\
\frac{dI_{r_h}}{dt} &= \psi\nu_h E_h - \gamma_h I_{r_h} \\
\frac{dI_h}{dt} &= (1-\psi)\nu_h E_h - \gamma_h I_h \\
\frac{dR_h}{dt} &= \gamma_h I_{r_h} + \gamma_h I_h \\
\frac{dS_v}{dt} &= \mu_v N_v - \lambda_v(t)S_v - \mu_v S_v \\
\frac{dE_v}{dt} &= \lambda_v(t)S_v - \nu_v E_v - \mu_v E_v \\
\frac{dI_v}{dt} &= \nu_v E_v - \mu_v I_v.
\end{aligned}\right\} \tag{1}$$

The population state variables are described within Table 1 and parameters are presented in Table 2. The quantities N_h and N_v represent the total populations of humans and mosquitoes within the model, and remain constant. We note that the equation for the evolution of $R_h(t)$ decouples from the system, as it is determined merely by computing the remaining population values.

2.1. Basic reproductive number

We define the basic reproductive number, $\mathcal{R}_0$, as the expected number of secondary infections by a single infectious individual over the duration of the infectious period within a fully susceptible population (Manore et al., 2014). As there is more than one class of infectives involved, we utilize the next generation method to derive an explicit formula for $\mathcal{R}_0$, defined mathematically by the spectral radius of the next generation matrix (Diekmann et al., 1990). We follow the process in Van den Driessche and Watmough (2002). Hence, we calculate the reproductive number as:

$$\mathcal{R}_0 := \rho(FV^{-1}) = \frac{\sigma_v\sqrt{N_v\beta_{hv}\beta_{vh}\nu_v}}{\sqrt{N_h\gamma_h\mu_v(\mu_v+\nu_v)}} = \sqrt{R_{hv}R_{vh}}$$

where $\rho(A)$ represents the spectral radius of the matrix A, and we have defined the quantities $R_{hv} = \left(\frac{\nu_v}{\mu_v+\nu_v}\right)\left(\frac{\sigma_v}{\mu_v}\right)\beta_{hv}$ and $R_{vh} = \left(\frac{N_v}{N_h}\right)\left(\frac{\sigma_v}{\gamma_h}\right)\beta_{vh}$. Details of this calculation can be found in the Appendix.

3. Incidence rates and parameter estimation

Although a common approach when modeling disease dynamics is to assume the total population within a country is susceptible, we deviate from this convention. Specifically, we assume the susceptible population depends on the biology and binomics of the *Aedes* species as well as the country's geography and uniquely calculate the at-risk population (described in the following section). We then use the at-risk population as the size of the initial susceptible population within simulations. While the deterministic model (1) captures the dynamics of the epidemic, we follow the opinion of the authors in Elderd et al. (2006), namely that more attention should be paid to how uncertainty in parameter estimates might affect model predictions. Thus, in Section 3.2, we focus on incorporating and quantifying the uncertainty of the disease process and the parameter values by means of embedding the deterministic model into a stochastic process.

3.1. Calculated at-risk population

The data utilized herein was reported by the Pan American Health Organization (PAHO) (Pan American Health Organization, 2016a,b), and is given by the number of cases, both confirmed and suspected, of Zika per week at the country level for Colombia, El Salvador and Suriname. Simulations performed by using the entire country population as the number of initially susceptible humans mischaracterized the disease dynamics, leading to overestimates in the final size of an epidemic, see Appendix (Fig. 12). One goal of this study is to identify the reporting rate for each country. However, only the product of the reporting rate and the susceptible population is identifiable (Eisenberg et al., 2013; Evans et al., 2005; Chapman and Evans, 2009). Thus, we choose to calculate a reasonable at-risk population rather than fitting the initial at-risk population to the data as a parameter. Since dengue and Zika occur in the same areas, share a common vector and have similar asymptomatic rates, we calculate the at-risk population size per country for a Zika outbreak based on historical data for dengue from 1995 to 2015 within Colombia, El Salvador, and Suriname (Pan American Health Organization, 2016a,b). Characteristics of Zika are largely unknown to date, thus other studies have also approximated Zika-specific values with known dengue-specific values (Funk et al., 2016; Perkins et al., 2016). The year of highest incidence for dengue provides an approximation for the number of susceptible individuals in a fully naïve at-risk population, which coincides with the dynamics of a newly emerging pathogen, such as Zika, that would spread rapidly in a completely susceptible population. We do not assume that the at-risk population for Zika is the same as the size of the largest dengue outbreak, but rather that it is *proportional* to the largest dengue outbreak. Thus we hold the parameters at constant baseline values (see Table 5) to run simulations of Zika Model (1) and obtain a reasonable at-risk population count for the number of initial susceptible individuals with regards to the first Zika wave in each considered country. Within each of the three

Table 2
Description of parameters within the Zika model. Dimensions are provided in parentheses on the right most side of the table.

σ_v	Number of times a single mosquito bites a human per unit time. The average number of days between bites is $1/\sigma_v$.	(Time^{-1})
β_{hv}	Probability of pathogen transmission from an infectious mosquito to a susceptible human given that a contact between the two occurs.	(Dimensionless)
β_{vh}	Probability of pathogen transmission from an infectious human to a susceptible mosquito given that a contact between the two occurs.	(Dimensionless)
ν_h	Per capita rate of progression of humans from the exposed state to the infectious state. The average duration of the latent period is $1/\nu_h$.	(Time^{-1})
γ_h	Per capita recovery rate for humans from the exposed state to the infectious state. The average duration of the infectious period is $1/\gamma_h$.	(Time^{-1})
ψ	Proportion of the infected human population that is reported.	(Dimensionless)
ν_v	Per capita rate of progression of mosquitoes from the exposed state to the infectious state. The average duration of the extrinsic incubation period is $1/\nu_v$.	(Time^{-1})
μ_v	Density-independent death rate for mosquitoes. The average lifespan of a mosquito is $1/\mu_v$.	(Time^{-1})
λ_h	The force of infection from infected mosquito to susceptible human. This is defined as (# of bites per human by mosquitoes per day) $\times$ (prob. a human is bitten by an infectious mosquito) $\times$ (prob. transmission occurs | a human was bitten by an infected mosquito) $= (\sigma_v \frac{N_v}{N_h})(\frac{I_v}{N_v})(\beta_{hv}) = \frac{\sigma_v \beta_{hv} I_v}{N_h}$.	(Time^{-1})
λ_v	The force of infection from infected mosquito to susceptible human. This is defined as (# of bites on a human per mosquito per day) $\times$ (prob. a mosquito bites an infected human) $\times$ (prob. transmission occurs | the mosquito bit an infected person) $= (\sigma_v)(\frac{I_h + I_{r_h}}{N_h})(\beta_{vh}) = \frac{\sigma_v \beta_{vh}(I_h + I_{r_h})}{N_h}$.	(Time^{-1})

Table 3
Reported dengue values from WHO used to compute the at-risk population.

Country	Highest incidence rate	Year	Reported number of cases
Colombia	0.00342	2010	157,152
El Salvador	0.00875	2014	53,460
Suriname	0.00580	2005	2,853

countries, the at-risk population value is strictly less than the total country population.

Table 3 indicates the year with the highest incidence rate and the reported number of cases for that year in each country of interest. See the Appendix (Fig. 13) for all historical data on dengue incidence rates for Colombia, El Salvador and Suriname.

We simulated Model (1) using the ode45 solver in MATLAB with chosen baseline parameter values (Table 5) while assuming that a single infectious human exists at the start of the epidemic. The at-risk population size for Colombia is 2.75 times the number of reported dengue cases from 2010. We estimated the multiplier for the at-risk population based on the best fit for the Zika epidemic. The at-risk population size for El Salvador is 1.425 times the number of reported dengue cases from 2014, while the at-risk population size for Suriname is 7.75 times the number of reported dengue cases from 2005. The variations between the values of the at-risk population for each country reflects its dependence upon the total population within each country as well as the dependence of the spread of the disease upon environmental factors. It is not expected that each country would have the same number of people at-risk of contracting Zika when the population densities and geography of each country also varies. There is no known data about absolute mosquito abundance in the regions considered, so we chose a reasonable mosquito to human ratio of 2:1 that is similar to values used in other studies (Manore et al., 2016, 2014; Kucharski et al., 2016; Funk et al., 2016). When starting our analysis with only one infected human, the simulated epidemic takes several weeks to ramp up to a detectable (reportable) level. If we begin simulations on the first day that a case is reported, the simulated peak occurs after the reported peak. Thus, we use shifted initial conditions (Table 4) that correspond to the population state sizes obtained approximately on day 38, 118, and 50 from the original simulation using Model (1) of the epidemics in Colombia, El Salvador and Suriname, respectively. We then repeat the process of simulating Model (1) using the shifted initial conditions to obtain solutions for the number of reported cases whose peak reporting weeks align more closely in time with that of the data. The precise values of the shifted initial conditions for each country, found in Table 4, are of the form $[S_h, E_h, I_{r_h}, I_h, R_h, S_v, E_v, I_v]$.

The number of reported cases from our simulations, using the calculated at-risk population and shifted initial conditions, are compared to the PAHO Zika data in Fig. 2. The solutions, which are similar to the data in peak and general shape, identify reasonable initial conditions. Although the baseline parameter values used in these simulations and the associated ranges are considered biologically reasonable, it is unknown which values within these ranges are most accurate. To obtain an expected value for a given parameter and describe the associated uncertainty within this quantity, the initial conditions will now be considered known (see Table 4) as we embed the deterministic Model (1) into a stochastic process enabling statistical inference in regards to parameter values. This process is described in Section 3.2.

Table 4
Computed at-risk population and other initial conditions.

Country	Original initial conditions	Shifted initial conditions[a]	ψ
Colombia	[432168, 0, 1, 0, 0, 864336, 0, 0]	[432163, 1, 0, 1, 4, 864330, 3, 3]	18%
El Salvador	[76181, 0, 1, 0, 0, 152362, 0, 0]	[75802, 87, 14, 62, 217, 152082, 145, 135]	18%
Suriname	[22111, 0, 1, 0, 0, 44222, 0, 0]	[22099, 3, 0, 2, 7, 44212, 5, 5]	22%

[a] The shifted initial conditions were obtained approximately from Day 38, 118, and 50 of the solution using the original initial conditions for Colombia, El Salvador and Suriname, respectively.

Table 5
Ranges and chosen baseline values for model parameters.

Parameter	Baseline	Range	Reference
$1/\sigma_v$	3.85	2–5.26	(Delatte et al., 2009; Sivanathan, 2006; Manore et al., 2016)
β_{hv}	0.54	0.1–0.75	(Manore et al., 2014, 2016; Kucharski et al., 2016)
$1/\nu_h$	6	3–12	(Campos et al., 2015; Foy et al., 2011; Fonseca et al., 2014; Kucharski et al., 2016; Lessler et al., 2016; Venturi et al., 2016; World Health Organization, 2016; Manore et al., 2016)
$1/\gamma_h$	7	3–14	(Campos et al., 2015; Foy et al., 2011; Fonseca et al., 2014; Kucharski et al., 2016; Lessler et al., 2016; Venturi et al., 2016; World Health Organization, 2016; Manore et al., 2016)
ψ	0.18	0.05–0.3	(Kucharski et al., 2016; Duffy et al., 2009; Manore et al., 2016)
β_{vh}	0.75	0.1–0.75	(Manore et al., 2014, 2016; Kucharski et al., 2016)
$1/\nu_v$	10.2	4.5–17	(Kucharski et al., 2016; Wong et al., 2013; Andraud et al., 2012; Boorman and Porterfield, 1956; Manore et al., 2016)
$1/\mu_v$	18	8–35	(Andraud et al., 2012; Otero et al., 2006; Fay, 1964; Manore et al., 2016)

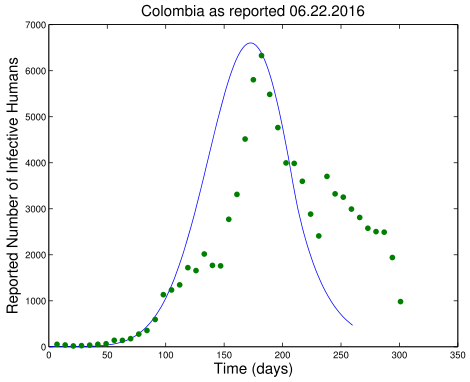

(a) Colombia - Model (1) initially fits the data well but was unable to capture the dynamics observed towards the end of the epidemic.

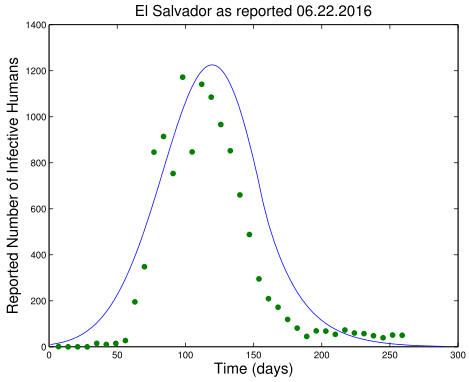

(b) El Salvador - Model (1) is able to capture the overall pattern of the epidemic but with a slightly later peak week.

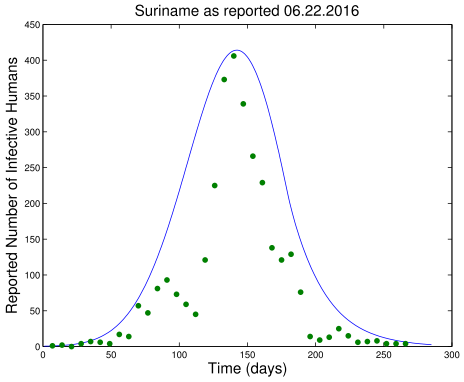

(c) Suriname - Model (1) is able to capture the overall pattern of the epidemic.

Fig. 2. Solutions of Model (1) obtained using the computed at-risk population (see shifted initial conditions Table 4) and constant baseline parameter values (Table 5) are plotted in blue along with the weekly Zika data available from PAHO shown as green circles. (a) Columbia: cases of Zika were reported first in Colombia on Epidemiological Week (EW) 32 of 2015. (b) El Salvador: the first Zika cases were reported on EW 38 of 2015. (c) Suriname: the reporting Zika cases began on EW 37 of 2015. (For interpretation of the references to color in this figure legend, the reader is referred to the web version of this article.)

3.2. An embedded stochastic model

Previous literature has provided biologically relevant parameter ranges (see Table 5) for the model. However, to obtain insight as to the distribution of these parameters across their ranges, we embed the deterministic system of ordinary differential equations (1) within a discrete-time stochastic process to obtain a corresponding stochastic model ((2), (3)) and perform an analysis in a Bayesian paradigm. We hold the data to be true and use the data to obtain an understanding of the dynamics which caused these epidemics to occur as they did. However, given that the data are collected by means that could cause inaccuracies, such as misdiagnosis for example, we do not take the approach of point estimation for each parameter value. Instead, we incorporate the uncertainty of the dynamics of the outbreak within our parameter estimation by calculating distributions of each parameter of interest. This approach adds a probabilistic component to both the contact/infection process and the disease progression process by capturing uncertainty at each modeling stage, rather than just within the contact/infection process (King et al., 2015). Therefore, embedding deterministic models into stochastic processes serves to (a) create a stochastic model informed by population-level

dynamics which includes uncertainty in the entire disease process rather than just due to data collection, (b) more adequately capture uncertainty present in the modeling framework, which is particularly important in small to medium sized epidemics, and (c) provide a convenient framework for fast computation of model parameters. The process by which we embed Model (1) into a stochastic process, (Mode and Sleeman, 2000), is summarized in the following paragraphs.

Previously, we obtained specific rates for the transfer of both humans and mosquitoes between their respective compartments, and these can be used to inform the stochastic analogues of these parameters. Throughout, we impose that the new model be conservative, i.e. $S_h + E_h + I_{r_h} + I_h + R_h = N_h$ and $S_v + E_v + I_v = N_v$ where N_h and N_v are the total human and mosquito populations, respectively. The assumption of conservation within the human population is plausible as the time span of the epidemic is much smaller than the average lifespan of a human. We hold the mosquito population as constant for the convenience of calculations and analysis. To approximate a continuous SEIR type model, we account for all events/transitions that may occur during time interval $(i, i+h_i]$ to be assigned to the related compartment on day i. Thus, the rate of change for a given population size can be approximated by the difference between the previous and current time steps. The model now takes the form

$$\left.\begin{aligned}
S_{i+h_i} &= S_i - E^*_{i+h_i}\\
E_{i+h_i} &= E_i + E^*_{i+h_i} - I^*_{i+h_i}\\
Ir_{i+h_i} &= Ir_i + \psi I^*_{i+h_i} - RIr^*_{i+h_i}\\
I_{i+h_i} &= I_i + (1-\psi) I^*_{i+h_i} - RI^*_{i+h_i}\\
R_{i+h_i} &= R_i + RIr^*_{i+h_i} + RI^*_{i+h_i}\\
Sv_{i+h_i} &= Sv_i + dEv^*_{i+h_i} + dIv^*_{i+h_i} - Ev^*_{i+h_i}\\
Ev_{i+h_i} &= Ev_i + Ev^*_{i+h_i} - Iv^*_{i+h_i} - dEv^*_{i+h_i}\\
Iv_{i+h_i} &= Iv_i + Iv^*_{i+h_i} - dIv^*_{i+h_i}.
\end{aligned}\right\} \quad (2)$$

We index time by i, and the temporal offset, h_i, which may not be constant but is known. All quantities represent counts and quantities denoted by an asterisk represent transition counts. In regards to the terms $\psi I^*_{i+h_i}$ and $(1-\psi)I^*_{i+h_i}$, the parameter ψ may yield values which are not integer counts. To be more liberal with the reporting size we calculated the smallest integer not less than the corresponding value of $\psi I^*_{i+h_i}$. To be more conservative with under-reporting size we calculated the largest integer not greater than the corresponding value of $(1-\psi)I^*_{i+h_i}$. When individuals can transition into a compartment via multiple routes, (e.g., recovered individuals can recover either with or without being reported as infected, $RIr^*_{i+h_i}$ and $RI^*_{i+h_i}$), two letters are used to denote the transition. In these cases, the first letter denotes *to which* compartment the individual transitions and the second denotes the compartment *from which* the individual transitions. The transition compartments which represent birth/death counts of the mosquito population on day $i+h_i$ are denoted, $dEv^*_{i+h_i}$ and $dIv^*_{i+h_i}$. Note that these values are drawn based on the calculated population sizes at time $i+h_i$. The compartments are labeled as follows: S – susceptible humans, E – latently infected humans, Ir – infectious reported humans, I – infectious unreported humans, R – recovered humans, Sv – susceptible mosquitoes, Ev – latently infected mosquitoes, Iv – infectious mosquitoes. Finally, the stochastic components of the model are given by

$$\left.\begin{aligned}
E^*_{i+h_i} &\sim \text{Bin}(S_i, 1-\exp(-\lambda_h h_i)),\ I^*_{i+h_i} \sim \text{Bin}(E_i, 1-\exp(-\nu_h h_i))\\
RIr^*_{i+h_i} &\sim \text{Bin}(Ir_i, 1-\exp(-\gamma h_i)),\ RI^*_{i+h_i} \sim \text{Bin}(I_i, 1-\exp(-\gamma h_i))\\
Ev^*_{i+h_i} &\sim \text{Bin}(Ev_i, 1-\exp(-\lambda_v h_i)),\ Iv^*_{i+h_i} \sim \text{Bin}(Iv_i, 1-\exp(-\nu_v h_i))\\
dEv^*_{i+h_i} &\sim \text{Bin}(Ev_{i+h_i}, 1-\exp(-\mu_h h_i)),\ dIv^*_{i+h_i} \sim \text{Bin}(Iv_{i+h_i}, 1-\exp(-\mu_h h_i)).
\end{aligned}\right\} \quad (3)$$

4. ABC algorithm and computation

Previous investigations (Duffy et al., 2009; Manore et al., 2014; Kucharski et al., 2016; Wong et al., 2013; Manore et al., 2016) have established biologically accepted ranges for the parameters $\boldsymbol{\Theta} = [\sigma_v, \beta_{hv}, \nu_h, \psi, \beta_{vh}, \nu_v, \mu_v]$ used within (1), but the conversion of model (1) to model ((2), (3)) will incorporate uncertainty into the disease process, and thus the values of these parameters. The stochastic model ((2), (3)) also allows for Bayesian inference on parameter posteriors which have the form

$$f(\boldsymbol{\Theta}|Y) \propto f(Y|\boldsymbol{\Theta})\pi(\boldsymbol{\Theta})$$

where $f(Y|\boldsymbol{\Theta})$ is the stochastic data model, which for fixed values of $\boldsymbol{\Theta}$ can be used to generate the random epidemic process, and $\pi(\boldsymbol{\Theta})$ is the prior distribution of the parameters. Thus, given both the data model and the prior distribution, we are able to calculate the posterior distribution $f(\boldsymbol{\Theta}|Y)$ up to a proportionality constant. This serves to update the distribution of the biologically accepted parameter ranges based on the actual epidemic data which we denote as Y.

The data model is constructed as a product of binomial probability density functions with different sample sizes and probabilities across every time point. See the Appendix for the precise formulation. Determining a Maximum Likelihood Estimate (MLE) to provide a point estimate and standard deviation for parameters may provide estimates outside of the valid biological ranges. In SEIR models, Markov Chain Monte Carlo (MCMC) methods produce parameter autocorrelations in chains which becomes problematic for tuning. We can avoid these obstacles by using Approximate Bayesian Computation (ABC). This method was introduced by Rubin et al. (1984) to obtain an approximation of the true posterior distribution, $f(\boldsymbol{\Theta}|Y)$. We also maintain the ability to trivially parallelize the simulations by choosing ABC over Sequential Monte Carlo (SMC). ABC samples from the posterior by randomly selecting parameter values from the prior that could adequately generate the data. In particular, random draws, $\boldsymbol{\Theta}^*$, from the prior distribution produce generated data sets, X, which are then compared to a given epidemic data set, Y, by means of a chosen distance metric, $\rho(X, Y)$. Those values of $\boldsymbol{\Theta}^*$ that generate data sets which fit the given data will be accepted as valid draws from the posterior distribution, and this implicitly conditions the posterior on Y. The algorithm of the computation is as follows, where N is the total number of accepted generated data sets X:

For $j \leq N$

1. Draw $\boldsymbol{\Theta}^* \sim \text{Unif}(a_k, b_k)$, where (a_k, b_k) is the corresponding parameter range found in Table 6 for all $k = 1, \ldots, 7$.
2. Generate X, time series data of the number of reported infectives, from model ((2), (3))
3. Calculate fitness of data using $\rho(X, Y)$
4. Set $\boldsymbol{\Theta}_{[j]} \longleftarrow \boldsymbol{\Theta}^*$ if $\rho(X, Y) \leq \epsilon$ and set $j \longleftarrow j+1$ else return to Step 1.

The metric, $\rho(X, Y)$, is considered a distance between the generated data set, X, and the observed data set, Y, typically based on

Table 6
Ranges for prior uniform distributions.

Parameter	Range
$1/\sigma_v$	0.5–10
β_{hv}	0.01–1
$1/\nu_h$	2–20
$1/\gamma_h$	7
ψ	0.05–0.35
β_{vh}	0.01–1
$1/\nu_v$	4–20
$1/\mu_v$	7–50

Note: We expand the ranges given in Table 5 as these are educated approximations and there is uncertainty with regards to the true range of most of these parameters.

sufficient statistics of the parameter space $\boldsymbol{\Theta}$. If $\rho(X, Y)$ is small enough, i.e., $\rho(X, Y) \leq \epsilon$ for some fixed small value $\epsilon > 0$, then

$$f(\boldsymbol{\Theta}|\rho(X, Y) \leq \epsilon) \approx f(\boldsymbol{\Theta}|Y).$$

One often uses sufficient statistics in defining $\rho(X, Y)$. These are statistics for which the data distribution conditioned on the sufficient statistic is free of $\boldsymbol{\Theta}$ (e.g., the sufficient statistic contains all information about $\boldsymbol{\Theta}$ that the full data set contains). By definition, the full data set is a sufficient statistic for $\boldsymbol{\Theta}$. Since a sufficient statistic of lower dimension than the full data set cannot be readily computed for our model, we consider a point-wise envelope metric comparing point by point the L_1-norm at every time step. Thus, if every data point of X and Y is close, then it directly follows that any statistics computed from X and Y, including sufficient statistics, will also be close. For the ABC method, the exact posterior distribution of $\boldsymbol{\Theta}$ can be found by accepting the simulated data set in which $X = Y$. This is computationally infeasible, however, so we instead consider X, such that $\frac{X_t}{Y_t} \in (\epsilon_1, \epsilon_2)$ for all time steps t with a corresponding peak week (with regards to time and value) and epidemic duration to Y, as an acceptable epidemic. Thus defining our metric, $\rho(X, Y)$, using (ϵ_1, ϵ_2), occurrence of peak week and the number of new infections during peak week. We call (ϵ_1, ϵ_2) the *envelope of tolerance* around the observed data set, Y, which is a common method for assessing a stochastic SEIR model fit (Lekone and Finkenstädt, 2006; Porter and Oleson, 2013, 2016). In Fig. 3, the observed data set is compared to randomly generated data sets without calculating a metric for validation of the drawn parameter values. Fig. 3 shows that many randomly drawn and biologically accepted values of $\boldsymbol{\Theta}$ generate epidemic outcomes which have distinctly different characteristics than the observed epidemic. Conversely, Fig. 4 demonstrates that epidemic outcomes of the accepted $\boldsymbol{\Theta}^*$ values generate epidemics with similar characteristics to that of the observed epidemic in regards to the total number of new infections each day, peak week occurrence, and peak value. Fig. 4(b) and (c) show generated epidemics similar to the data in both peak and duration. Note that this does not occur in Fig. 4(a). The accepted parameter values obtained using the ABC method yield outbreaks which vary greatly in peak occurrence, leading us to conclude that the dynamics of the country-level data are different than those in the deterministic model. Therefore the ABC method does not generate infectious curves similar to the Colombia data. Fig. 4(a) was generated from acceptances using an envelope of (1/20, 20). A tighter envelope of (1/10, 10) was computed; however, the method ran for approximately 35 days to obtain the same number of acceptances as the (1/20, 20) envelope with no visible changes in the same plot as Fig. 4(a). Because acceptances for tighter envelopes are

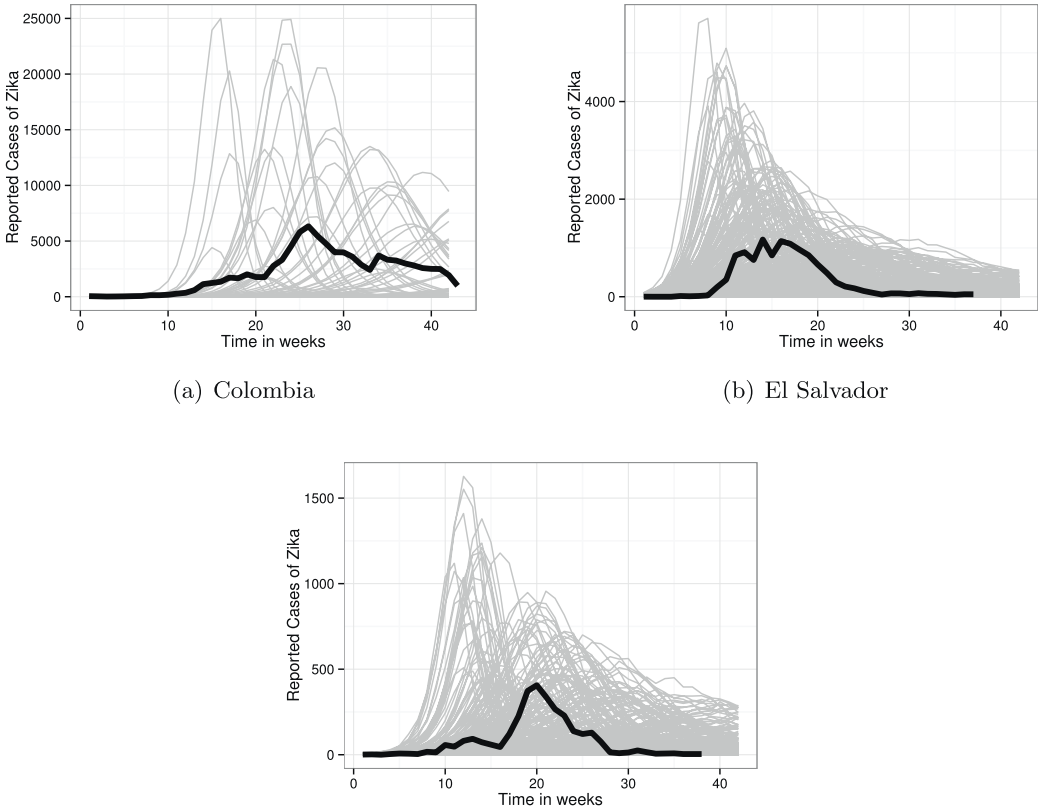

(a) Colombia

(b) El Salvador

(c) Suriname

Fig. 3. Each subfigure contains the results of using randomly drawn parameter vectors in model ((2), (3)) to generate outcomes of the epidemic in which a metric is not applied. For all three countries the biologically accepted parameter values (see Tables 5 and 6) generate epidemics that vary greatly from the characteristics of the observed epidemics, particularly in the peak and duration.

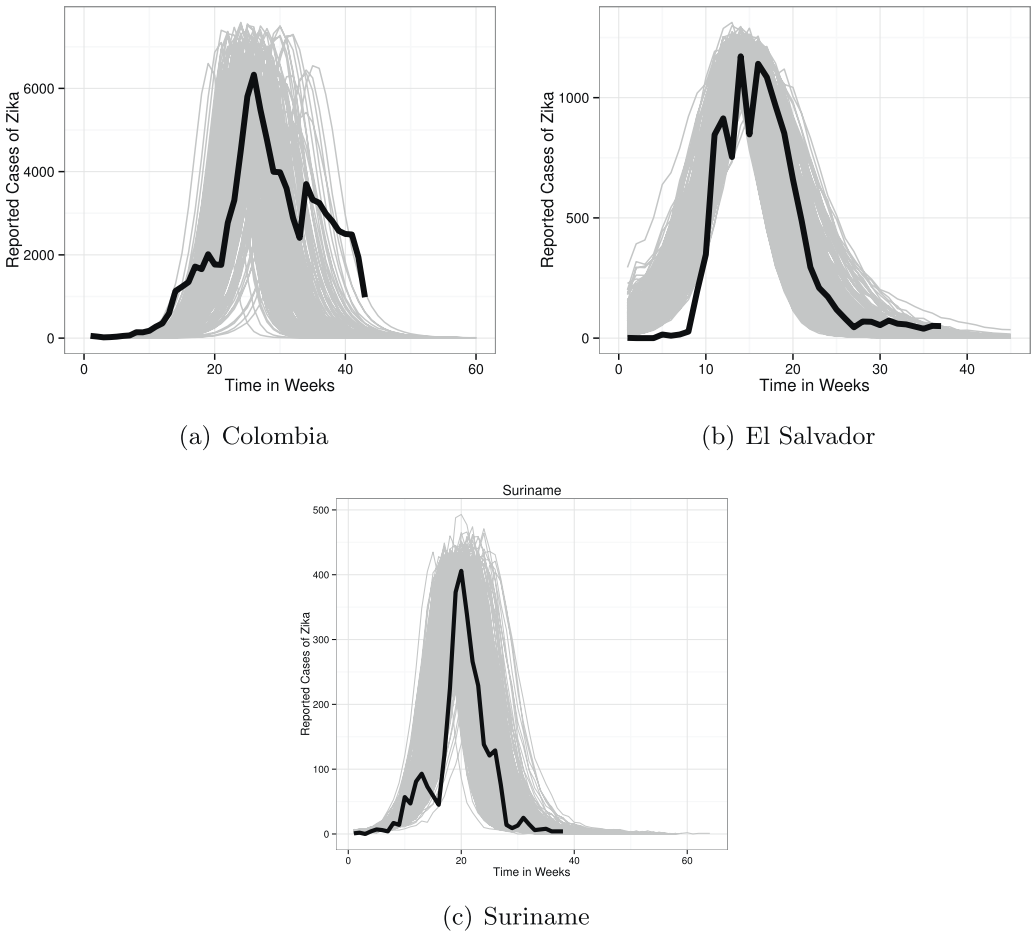

(a) Colombia (b) El Salvador

(c) Suriname

Fig. 4. Each subfigure compares the number of new infections reported each week of the generated epidemics (gray) calculated using model ((2), (3)) with 500 of the 10,000 accepted randomly generated parameter vector draws to the observed epidemic in each country (black). The envelope of tolerance is (1/20, 20) for Colombia (a) with the occurrence of peak week within ±4 weeks of the known peak week and the peak number of new infections less than or equal to a 20% deviation from the observed value. The envelope of tolerance for El Salvador (b) is (2/3, 3/2) with the occurrence of peak week within ±2 weeks of the known peak week and the number of new infections reported during peak week less than or equal to a 5% deviation from the observed peak value. The data from Suriname (c) was compared to generated data with an envelope of tolerance of (1/4, 4) and the occurrence of peak week within ±2 weeks of the known peak week and the number of new infections reported during peak week is less than or equal to a 5% deviation from the observed peak value.

not possible, we can conclude the model is improperly specified to capture the dynamics of Colombia at the country level. Reasons for this outcome are discussed in Section 6.

Fig. 5 depicts the effect of generating accepted epidemics with smaller and smaller envelopes of tolerance on the posterior distributions. We plot the kernel densities of both the reporting rate, ψ, and reproductive number, $\mathcal{R}_0$, distributions for El Salvador and Suriname. While only two parameters are shown here, the same observations are found in the kernel density plots of the other parameters of interest. We see in Fig. 5 that envelopes of various size produce similar but different kernel densities, with the tighter envelopes producing a more peaked density distribution. A slight shift in the peak of the kernel densities is observed in Fig. 5(a) and (d). This would indicate the need to shrink the envelope further to obtain an estimation that is closer to the true posterior distribution. However, attempts to generate data sets satisfying tighter envelopes could not produce acceptances, indicating that these envelope sizes are the best possible fits of the stochastic $SEI_TIRS_vE_vI_v$ model to the observed country-level data. Further analysis would require refining the dynamics of model (1) and model ((2), (3)) or using data at a more refined spatial scale.

5. Results

We assigned uniform distributions to the accepted biological ranges found in Table 6. After 10,000 acceptances from the ABC algorithm, the histograms and kernel densities for selected parameters from El Salvador are given in Figs. 6, 8, and 14 and Tables 7 and 11. Selected parameters from Suriname are given in Figs. 7, 8, and 15 and Tables 8 and 12. We estimated the basic reproduction number for El Salvador and Suriname, with median values of 2.0 and 2.3, respectively (Table 9 and Fig. 16). Fig. 9 displays the number of reported cases from the generated epidemics based on 10,000 accepted parameter values. The time series of the number of total cases during the generated epidemics of both reported and unreported infectives is found in Fig. 10 with reported cases and estimated total cases shown in Table 10. The histogram and kernel density plots of the total number of Zika virus cases, reported and unreported are shown in Fig. 11 (Tables 7–10).

6. Conclusions and discussion

Within the present study, a new stochastic model was formulated to describe the spread of the Zika virus within Colombia, Suriname, and El Salvador. The variability in per capita susceptibil-

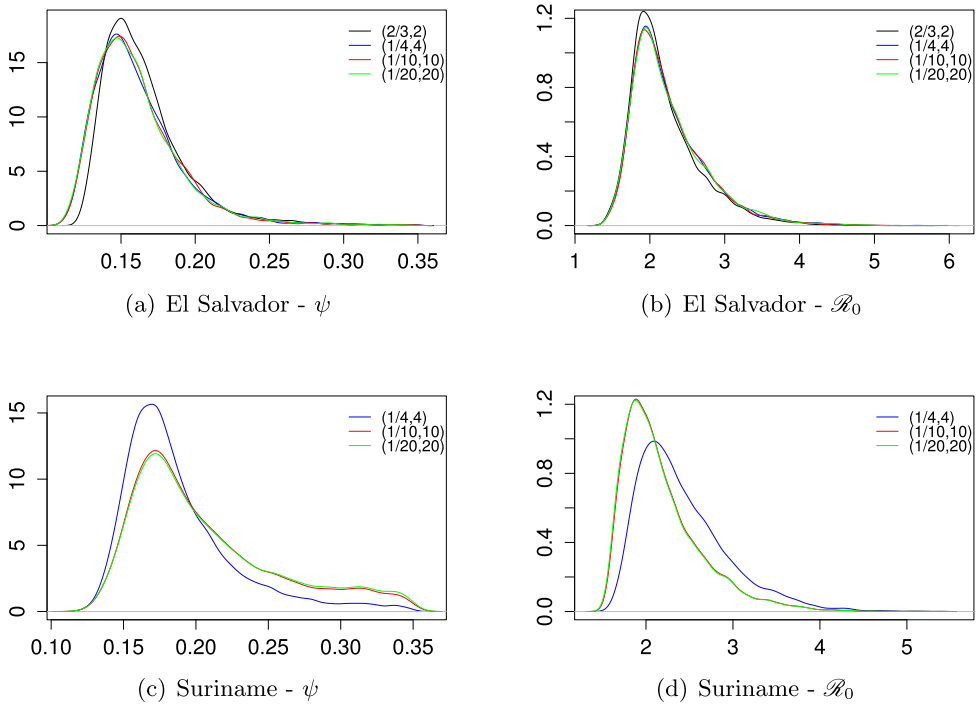

Fig. 5. Subfigures (a) and (c) display the kernel density plots of the proportion of reported infectious, ψ, with various envelope sizes for El Salvador and Suriname, respectively, while subfigures (b) and (d) show the kernel density plots of the reproductive number, $\mathcal{R}_0$ for El Salvador and Suriname, respectively. All generated data sets for which accepted values of ψ and $\mathcal{R}_0$ were found maintained an occurrence of peak week within ±2 weeks of the known peak week and the number of new infections reported during peak week less than or equal to a 5% deviation from the observed peak value. As the legends indicate, an envelope size of (2/3, 3/2) is displayed by the black curve, an envelope size of (1/4, 4) is displayed in blue, the red curve represents an envelope size of (1/10, 10), and similarly the green curves indicate an envelope size of (1/20, 20) using green. Note that envelopes of all four sizes were able to generate acceptances from the El Salvador data while the data from Suriname only allowed for acceptance to be generated from envelope sizes of (1/4, 4), (1/10, 10), and (1/20, 20). (For interpretation of the references to color in this figure legend, the reader is referred to the web version of this article.)

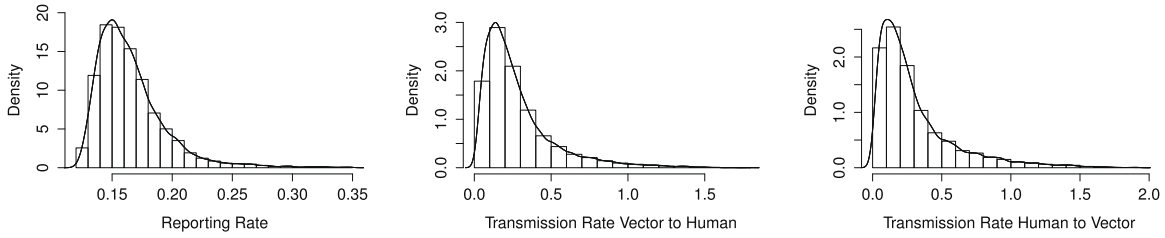

Fig. 6. ABC generated histograms and kernel density plots for the reporting rate, ψ, transmission rate for the human population, $\sigma_v\beta_{hv}$, and mosquito population, $\sigma_v\beta_{vh}$ in El Salvador.

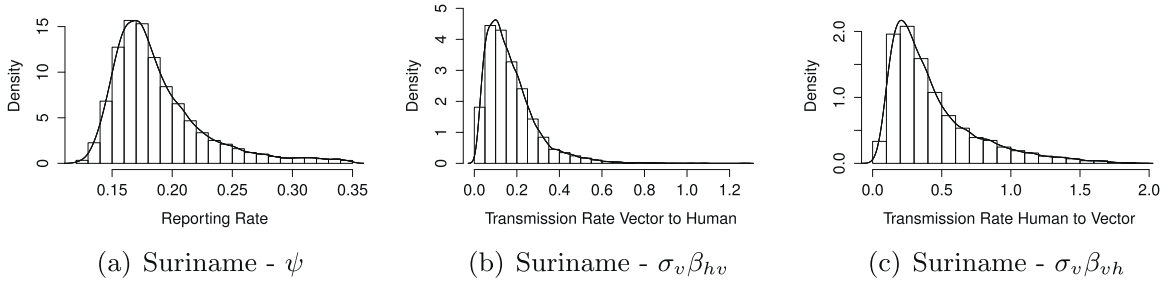

Fig. 7. ABC generated histograms and kernel density plots for the reporting rate, ψ, the force of infection for the human population, $\sigma_v\beta_{hv}$, and mosquito population, $\sigma_v\beta_{vh}$ in Suriname.

ity within each country was introduced by uniquely calculating the at-risk population based on historical data for dengue virus, whose epidemic characteristics are similar to that of Zika. The initial population state sizes based on this dengue data created similar values of weekly reported cases of Zika, both suspected and confirmed, using baseline values of parameters to evaluate model (1) to those reported by the PAHO. Once the at-risk population was estimated, the initial population state sizes for these nations were fixed to

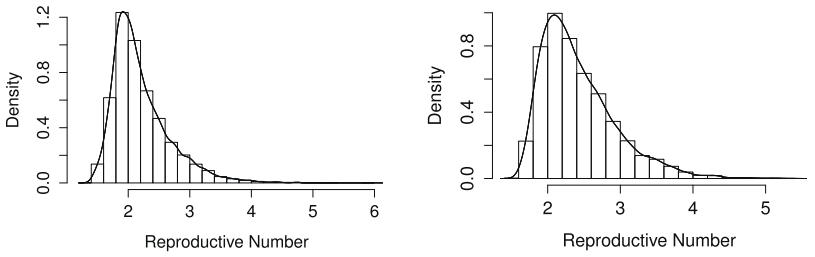

(a) El Salvador - $\mathscr{R}_0$ (b) Suriname - $\mathscr{R}_0$

Fig. 8. ABC generated histograms and kernel density plots of the reproductive number for El Salvador (a) and Suriname (b).

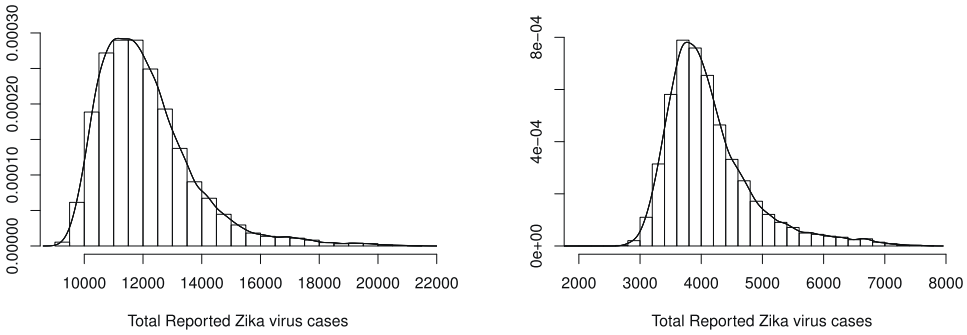

(a) El Salvador (b) Suriname

Fig. 9. Histogram with kernel density plot of the total number of reported Zika virus cases generated from the ABC accepted parameter values for El Salvador (a) and Suriname (b).

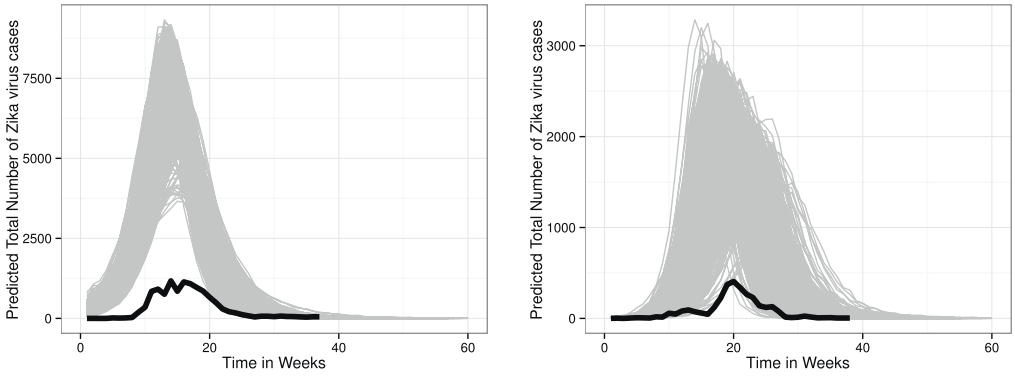

(a) El Salvador (b) Suriname

Fig. 10. Generated time series data (grey) for the total number of Zika cases (reported + unreported) from the ABC-accepted parameter values as compared to the observed data (black) reported by PAHO for El Salvador (a) and Suriname (b).

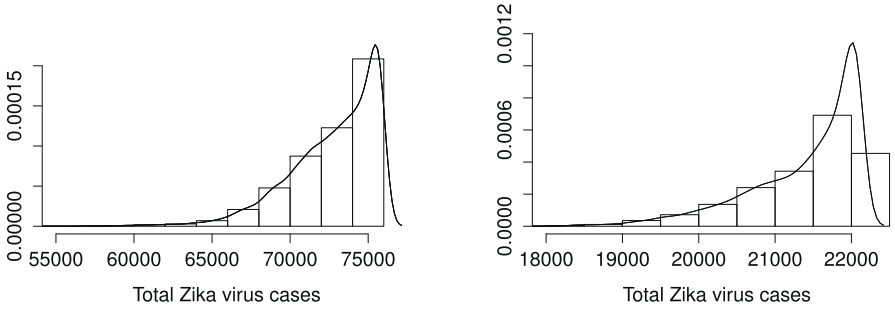

(a) El Salvador (b) Suriname

Fig. 11. Histogram and kernel density plot of generated total number of Zika virus cases, both reported and unreported, from the ABC accepted parameter values for El Salvador (a) and Suriname (b).

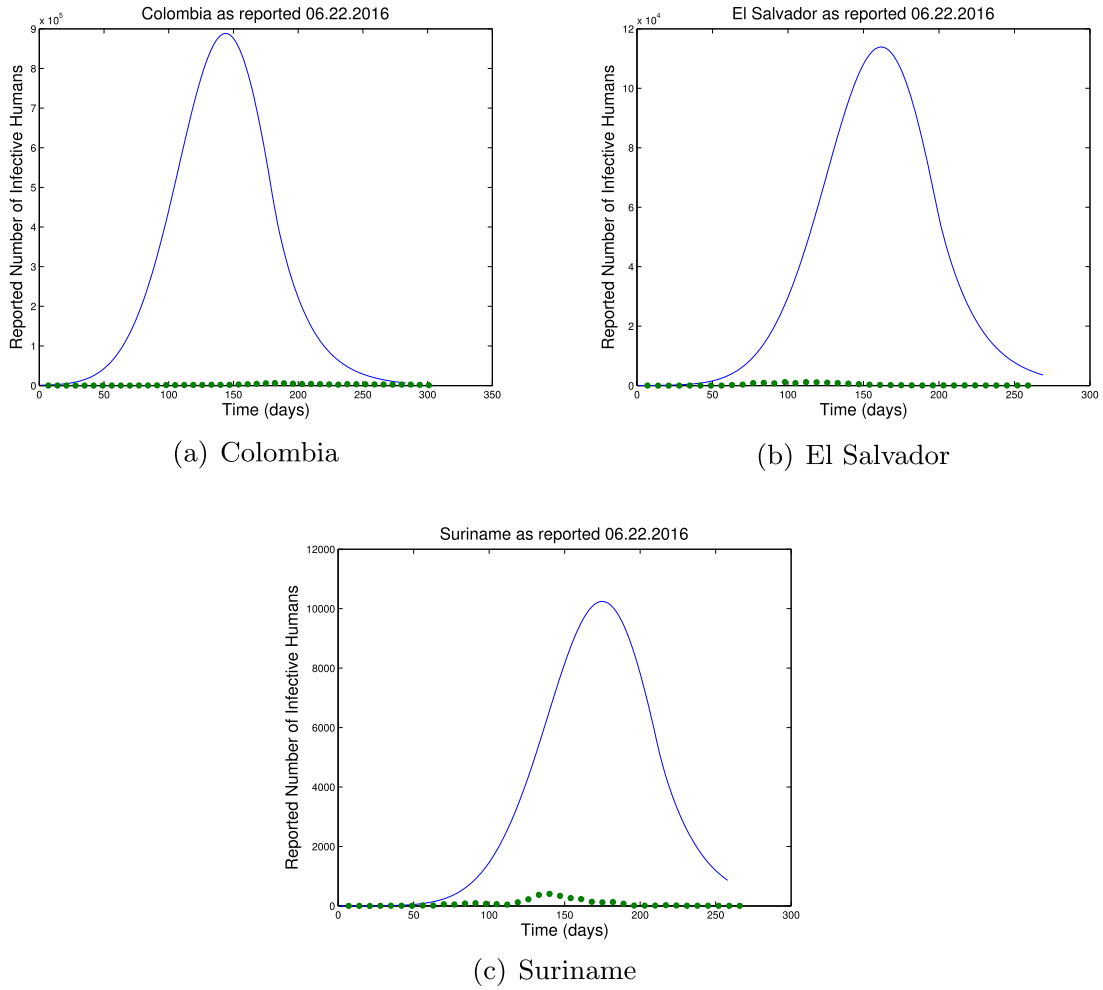

Fig. 12. The time series for the number of reported infectives as calculated using model (1) with the initial number of susceptible people equal to the total population (solid blue line) and baseline parameter values (Table 5) as compared to the PAHO data (dotted green) as reported 06.22.2016 per country. The total populations as reported for 2015 are 48,010,049 (Colombia), 6,117,145 (El Salvador), 540,612 (Suriname) accessed 6.22.16 at http://countrymeters.info/. (For interpretation of the references to color in this figure legend, the reader is referred to the web version of this article.)

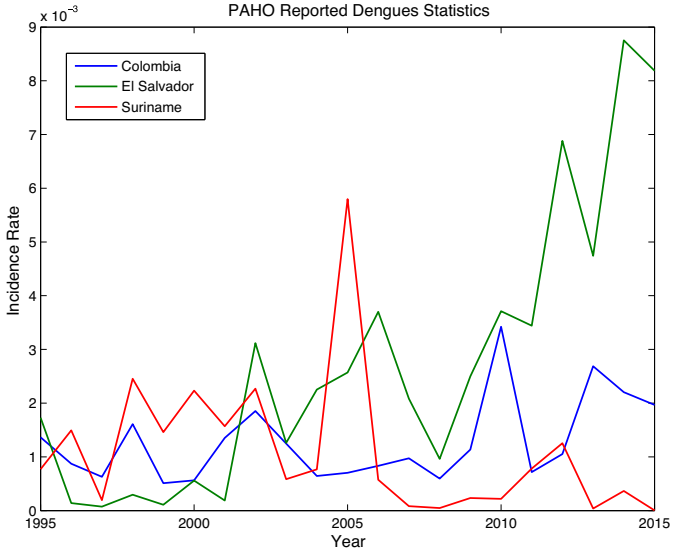

Fig. 13. Reported rates of incidence of dengue are calculated based on the number of reported cases documented (Pan American Health Organization, 2016a,b) divided by the reported country population in the corresponding year (Countrymeters, 2016).

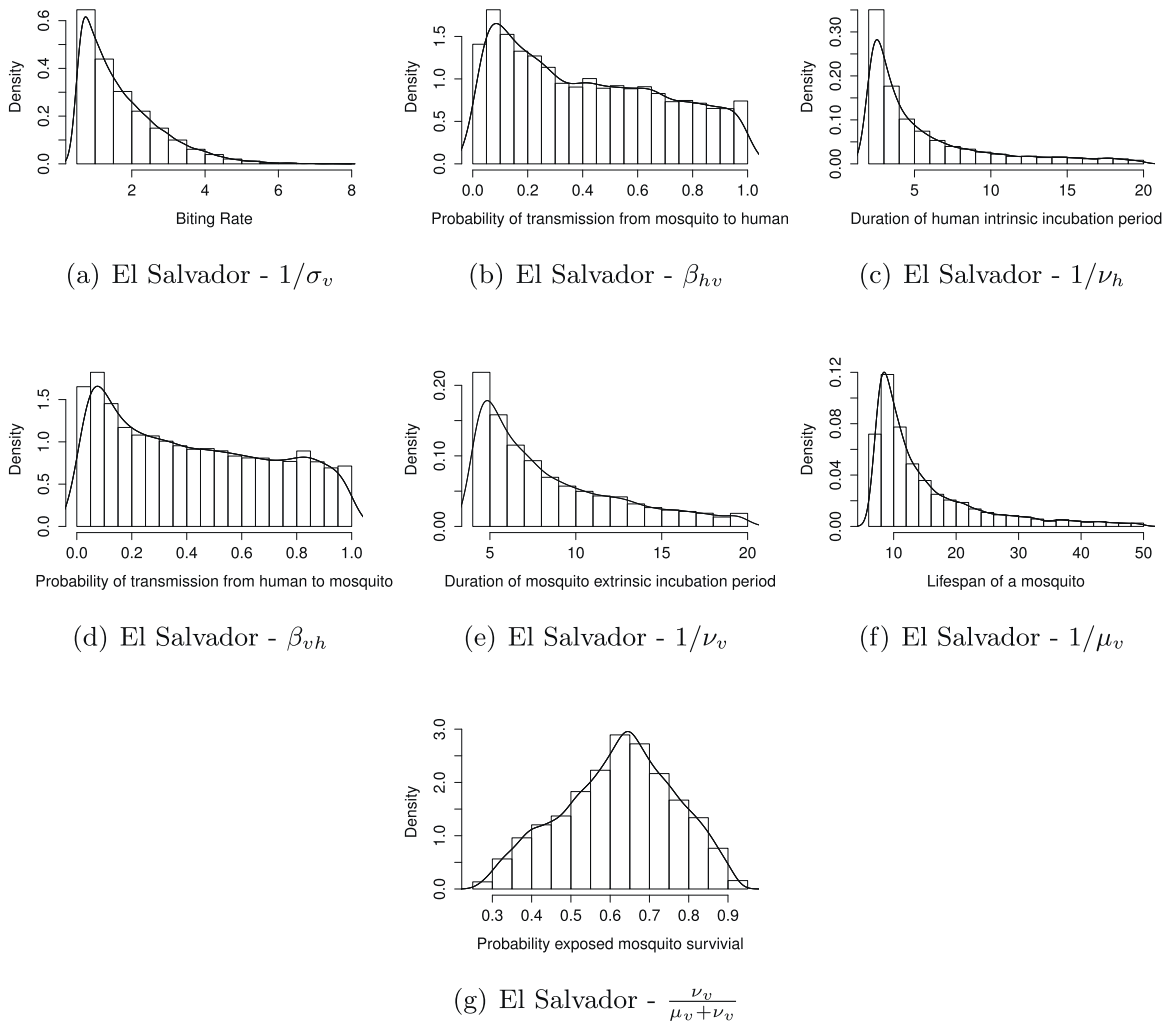

(a) El Salvador - $1/\sigma_v$ (b) El Salvador - β_{hv} (c) El Salvador - $1/\nu_h$

(d) El Salvador - β_{vh} (e) El Salvador - $1/\nu_v$ (f) El Salvador - $1/\mu_v$

(g) El Salvador - $\frac{\nu_v}{\mu_v+\nu_v}$

Fig. 14. Distributions for the remaining parameters used for modeling Zika dynamics in El Salvador.

Table 7
Selected parameter statistics for El Salvador and credible intervals (C.I.).[a]

	ψ	$\sigma_v\beta_{hv}$	$\sigma_v\beta_{vh}$
Mean	0.1654	0.2808	0.3053
Median	0.1593	0.2124	0.2130
Mode	0.1501	0.1372	0.1091
95% C.I.	[0.1248, 0.2205]	[0.0191, 0.7782]	[0.0119, 0.9244]

[a] Note: The credible interval, used in the Bayesian paradigm, summarizes the uncertainty by giving a range of values on the posterior probability distribution that includes 95% of the probability.

Table 8
Selected parameter statistics for Suriname and credible intervals.

	ψ	$\sigma_v\beta_{hv}$	$\sigma_v\beta_{vh}$
Mean	0.1877	0.1705	0.4352
Median	0.1777	0.1429	0.3365
Mode	0.1693	0.0998	0.2069
95% C.I.	[0.1304, 0.2717]	[0.0165, 0.4054]	[0.04287, 1.1241]

enable estimation of parameter values and obtain more informative distributions than the accepted uniform biological parameter ranges. The deterministic system (1) was embedded into a stochastic process to obtain a more general stochastic model ((2), (3)). For each of the three nations, an ABC algorithm was implemented using ((2), (3)) to compute approximate posterior distributions of the parameters conditioned on the data. By obtaining these pos-

Table 9
Reproductive number statistics per country and credible intervals.

$\mathcal{R}_0$	El Salvador	Suriname
Mean	2.2055	2.4225
Median	2.0854	2.3062
Median[2]	4.3487	5.3186
Mode	1.9174	2.0901
95% C.I.	[1.4664, 3.1658]	[1.6526, 3.4704]

Note: The median[2] is an approximation of the type of reproduction number (i.e. human-to-human) as opposed to $\mathcal{R}_0$, which is the single generation reproduction number.

Table 10
Statistics for the generated total cases (reported and unreported) per country and credible intervals.

	Reported cases	Total cases
El Salvador		
Mean	12107	72721
Median	11810	73395
Mode	11158	75457
95% C.I.	[9606,15321]	[67317, 75889]
PAHO data	11825	
Suriname		
Mean	4132	21390
Median	3975	21647.5
Mode	3758	22018
95% C.I.	[3013, 5697]	[19853,221027]
PAHO data	3042	

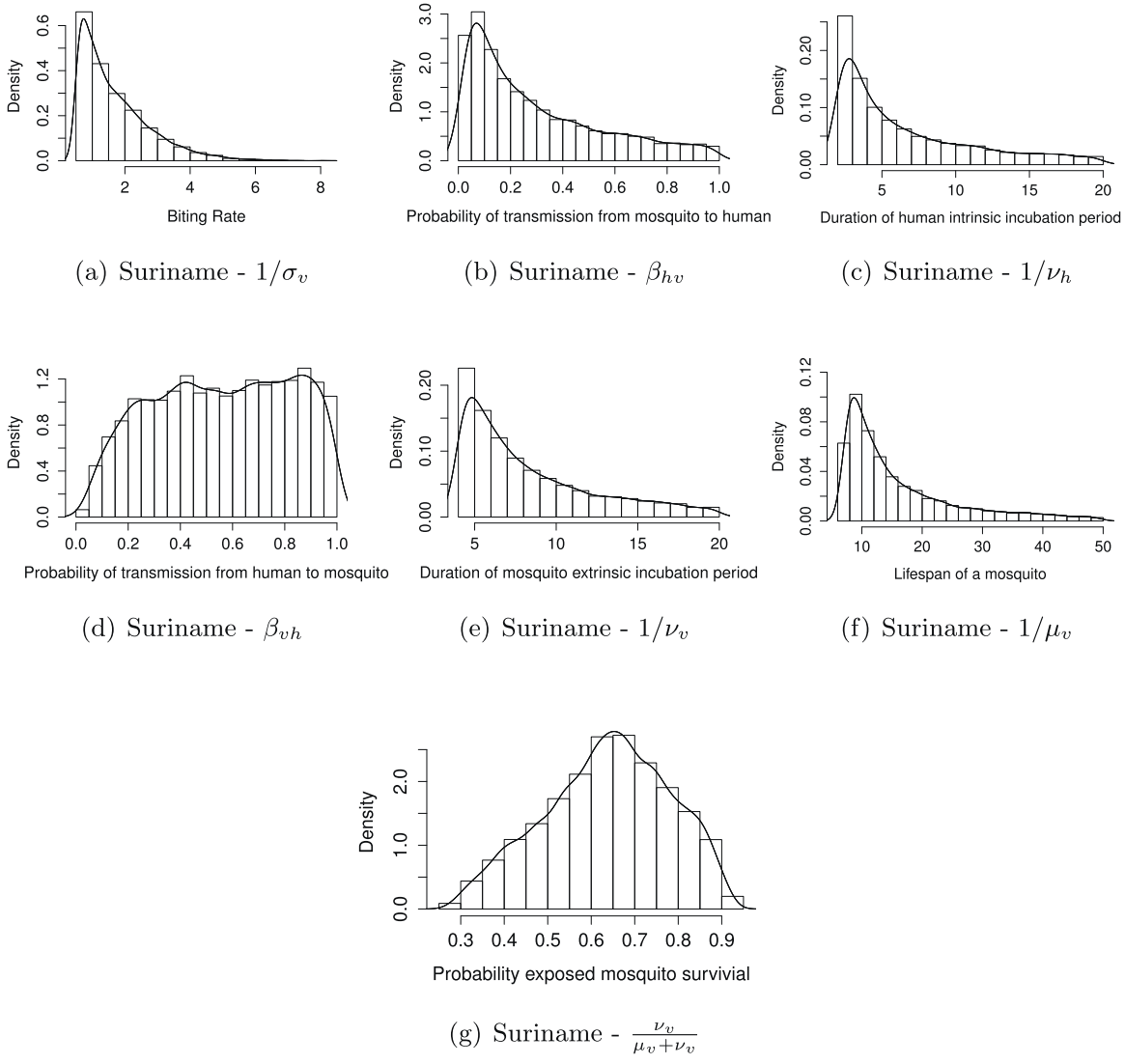

(a) Suriname - $1/\sigma_v$ (b) Suriname - β_{hv} (c) Suriname - $1/\nu_h$

(d) Suriname - β_{vh} (e) Suriname - $1/\nu_v$ (f) Suriname - $1/\mu_v$

(g) Suriname - $\frac{\nu_v}{\mu_v+\nu_v}$

Fig. 15. Distributions for the remaining parameters used for modeling Zika dynamics in Suriname.

terior distributions, the uncertainty in parameter values for each country can be quantified by way of informative statistics, such as the mean, mode, median and variance, to more accurately describe rates within the system.

Properties of the disease within El Salvador and Suriname were estimated by the model. Under these assumptions, El Salvador is estimated to have a mean reporting rate of 16.5% which is near the upper bound of the previous estimate of Kucharski et al. (2016) with a credible interval of [12.5%, 22%]. The mean values of the forcing terms, λ_h and λ_v, are approximately 0.28 and 0.31 with credible intervals of [0.0191, 0.7782] and [0.0119, 0.9244], respectively. Suriname has a mean reporting rate greater than the predicted interval of Kucharski et al. (2016) at 18.8% with a credible interval of [13%, 27%]. The forcing terms of Suriname, λ_h and λ_v, had mean values of 0.17 and 0.43 with credible intervals of [0.0165, 0.4054] and [0.0429, 1.1241], respectively. The basic reproductive number, $\mathcal{R}_0$, was defined such that ${\mathcal{R}_0}^2$ yields the number of secondary human infections within a fully susceptible population arising from a single new human infection. In Suriname, the mean value of ${\mathcal{R}_0}^2$ was 5.31, while the mean reproductive number was 4.35 in El Salvador. These quantities are similar to other predictions for the mean of ${\mathcal{R}_0}^2$ found in Nishiura et al. (2016), Towers et al. (2016), Villela et al. (2017).

Though this analysis has provided additional insight into the spread of the disease, our methods were unable to accurately estimate the aforementioned statistics for Colombia (see Section 4) as the ABC method was unable to be executed with tighter envelopes of tolerance. One possible reason for this could be the appearance of a second peak in the epidemic, see Fig. 2(a). While there is a distinct and large peak during EW 26, a smaller second peak occurs during EW 34. In contrast, the peaks which occur in the uncleaned data sets for El Salvador and Suriname do not inhibit the mathematical analysis. This is seen in the ability to compute similar generated data sets with tighter envelopes of tolerance (in Fig. 4 envelopes of tolerance for Suriname and El Salvador were much tighter than the envelope of tolerance for Colombia). Therefore, the peaks within these data sets are likely due to inaccuracies in reporting and not to an underlying misunderstanding of the dynamics of the epidemic. A possible explanation for the second peak in the Colombia data set may be a second outbreak in a disjoint location from the first outbreak. In particular, the extreme topographical variations within Colombia could lead to a delay in the spread of the disease across the entire country. Thus, we suggest that the epidemiological characteristics of Zika in Colombia should be studied at a more granular spatial level, differentiating amongst regions or even municipalities and cities.

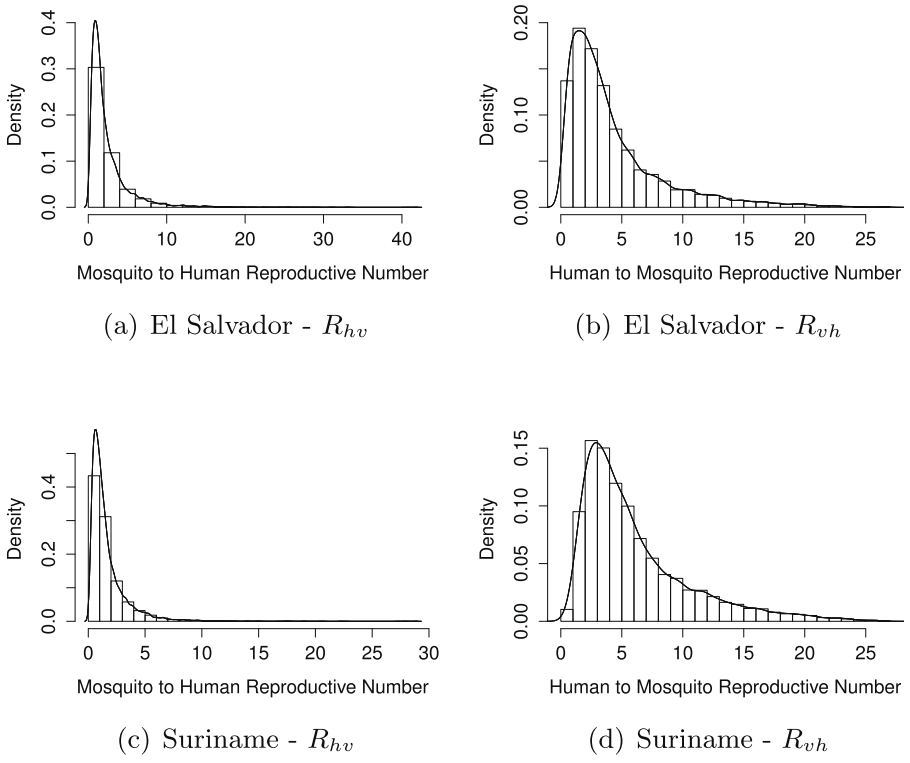

Fig. 16. Displayed are the type reproductive ratios. For El Salvador the mosquito to human ratio histogram and kernel density is (a) while the human to mosquito ratio histogram and kernel density is (b). (c) and (d) show the histogram and kernel density plots of the mosquito to human and human to mosquito ratios for Suriname, respectively.

Table 11
Statistics for the other parameter values for El Salvador and credible intervals.

	$1/\sigma_v$	β_{hv}	$1/\nu_h$	β_{vh}	$1/\nu_v$	$1/\mu_v$	$\frac{\nu_v}{\mu_v+\nu_v}$
Mean	1.6894	0.4201	5.5626	0.4260	8.4171	14.9655	0.6206
Median	1.3874	0.3817	3.8095	0.3882	7.0799	11.4532	0.6315
Mode	0.7397	0.0851	2.5506	0.0760	4.8253	8.4276	0.6451
95% C.I.	[0.5004, 3.8294]	[0.01274, 0.9302]	[2.0001, 15.5402]	[0.0104, 0.9289]	[4.0001, 17.0355]	[7.1432, 35.9220]	[0.3475, 0.8832]

Table 12
Statistics for the other parameter values for Suriname and credible intervals.

	$1/\sigma_v$	β_{hv}	$1/\nu_h$	β_{vh}	$1/\nu_v$	$1/\mu_v$	$\frac{\nu_v}{\mu_v+\nu_v}$
Mean	1.6819	0.3004	6.6144	0.5602	8.3111	16.1174	0.6369
Median	1.3684	0.2141	4.8592	0.5657	6.9234	12.4293	0.6453
Mode	0.7375	0.0702	2.7695	0.8657	4.8375	8.7023	0.6521
95% C.I.	[0.5002, 3.8328]	[0.0101, 0.8456]	[2.0001, 16.8145]	[0.1358, 0.9985]	[4.0000, 16.9617]	[7.1467, 38.2319]	[0.3699, 0.8961]

Table 13
Statistics for the type reproductive numbers and credible intervals.

	El Salvador – R_{hv}	El Salvador – R_{vh}	Suriname – R_{hv}	Suriname – R_{vh}
Mean	2.4588	4.2743	1.6667	6.0925
Median	1.5509	2.9813	1.1414	4.7115
Mode	0.9238	1.5273	0.6250	2.8961
95% C.I.	[0.1519, 7.4016]	[0.1663, 12.9415]	[0.1473, 4.8498]	[0.6002, 15.7379]

We also estimated the total number of infected people in El Salvador to be 72,721 (with an estimated 12,107 reported cases) and the total number of people infected in Suriname to be 21,390 (with an estimated 4132 reported cases). So, about 95% of the at-risk (high-risk) populations were infected by the end of the outbreak. The predicted *reported* country-level incidence for El Salvador is 0.0019 and for Suriname is 0.0073. However, the *true* country-level incidence for El Salvador is predicted to be 0.0119 while for Suriname it is 0.0396 assuming total populations of 6,117,145 and 540,612, respectively. From a public health perspective, our model indicates that about 6 times as many people were infected than were reported in El Salvador and 5 times as many were infected than were reported in Suriname. Depending on the percent of the at-risk population that was pregnant during the outbreak, our model suggests that a larger number of birth defects than indicated by the reported number of cases could be expected in these countries. Interestingly, although the values for the mosquito extrinsic incubation period and mosquito lifespan had relatively wide ranges even among mean, median, and mode values, the probability of a mosquito surviving the incubation period (Tables 12 and 13) was

quite similar across statistics and countries at about 65%. This corresponds to the extrinsic incubation period lasting around 1/2 of the average mosquito lifespan. A major difference between predicted parameter values for El Salvador and Suriname occurs in the transmission probabilities. While the values for β_{hv} and β_{vh} for El Salvador were similar (both estimated to be about 0.42), in Suriname, the mosquito-to-human probability of transmission, β_{hv} was consistently less than half that of the human-to-mosquito transmission, β_{vh}, with a median of 0.21 and 0.56, respectively. Since these terms capture many intrinsic uncertainties in the transmission process, it is hard to interpret the meaning of this difference. It could be an artifact of the model or could indicate a reduced efficiency of the mosquitoes in Suriname in passing on the virus.

In conclusion, our research provides important parameter estimates for the spread of Zika in El Salvador and Suriname, along with uncertainty quantification and credible intervals for those parameters. We estimated the basic and type reproduction numbers and the total number of people infected - quantities needed to inform assessments of economic cost and risk, among other factors. We found that the type reproduction number is higher in Suriname than in El Salvador, indicating a higher risk in Suriname. This could be explained by differences in climate between the two countries or in other socio-economic or geographic factors affecting mosquito-borne disease transmission. Additionally, our methods could be applied to other countries or regions experiencing outbreaks to estimate region-specific parameters and provide decision makers with important information about surveillance and control both at present and in the future. Another advantage of this method is that it can indicate what scale is appropriate for these calculations. For example, we found that a country-level analysis of the Colombia data was not appropriate. In the future, it would be interesting to apply the model to a regional Colombia data set.

The results in this paper are dependent on several assumptions. We assumed homogeneous mixing between the mosquito and the at-risk human populations as well as uniform susceptibility and infectivity. The parameters were considered to be time and space invariant. The total number of mosquitoes within the system was assumed to be constant and proportional to the number of at-risk humans. Depending on the levels of spatial and temporal heterogeneity at play during the Zika outbreak, our model could be under- or over-predicting the country-level parameters. While not directly proven, we assumed the human population to obtain lifelong immunity, or, functionally, immunity for the duration of the outbreak. The simulations performed herein were restricted to less than one year, making the immunity assumption reasonable. However, a long term predictive model would warrant further exploration of this assumption. Our model and results highlight the need for better data collection at varying spatial and temporal scales which could inform both human and mosquito related parameters. The estimates we present here can be verified or discounted by follow-up studies quantifying attack rate, observed birth defects, and Zika seroprevalence.

In future studies, the initial population state sizes obtained in the calculations of the respective at-risk populations could be considered parameters themselves. Hence, one could perform a statistical analysis on acceptable ranges for such initial values to quantify the uncertainty of these populations. For instance, this could be done by generating a posterior distribution for the initial susceptible population for each country, as well as the parameters in the system. Additionally, the mosquito population for each country was assumed to be constant for convenience. However, utilizing a more realistic model of the total mosquito population which changes in time (similar to the methods in Manore et al., 2014) may yield different results, and this would also be a suitable direction for future research. Finally, the recovery period, $1/\gamma_h$, was held constant in the current study due to the assumption that its mean value had been medically established. Still, another investigation using the methods developed herein, but considering a uniformly-distributed prior for the recovery period, may provide better insight into the distribution and expected value of this period. We conclude that additional studies are needed to fully understand Zika virus transmission dynamics. However, our research suggests that the reporting rates in El Salvador and Suriname are quite low and thus, additional surveillance systems may be needed to measure the true burden of Zika in these countries.

Acknowledgments

This work was supported by NSF SEES grant CHE-1314029, NSF RAPID (DEB 1641130), and NSF EDT grant DMS-1551229. SP was partially supported by NSF under grant DMS-1614586. SD was partially supported by NIH/NIGMS/MIDAS under grant U01-GM097658-01. LANL is operated by Los Alamos National Security, LLC for the Department of Energy under contract DE-AC52-06NA25396. Approved for public release: LA-UR-17-20963. The funders had no role in study design, data collection and analysis, decision to publish, or preparation of the manuscript.

Appendix A. Results of model (1) using total country populations as the initial size susceptible populations

A.1 Results of model (1) using total country populations as the initial size susceptible populations

A.2 Basic reproductive number

We define the basic reproductive number, $\mathcal{R}_0$, as the expected number of secondary infections by a single infectious individual over the duration of the infectious period within a fully susceptible population (Manore et al., 2014). As there is more than one class of infectives involved, we utilize the next generation method to derive an explicit formula for $\mathcal{R}_0$, defined mathematically by the spectral radius of the next generation matrix (Diekmann et al., 1990). We follow the process in Van den Driessche and Watmough (2002) and define $\mathbf{x} = [E_h, I_{r_h}, I_h, E_v, I_v, S_h, R_h, S_v]^T$; thus reordering the presentation of populations from the original system to ensure our calculations possess the correct biological representation. Let $\mathcal{F}_i(x)$ be the rate of appearance of new infections in compartment i. We indicate the rate of transfer of individuals out of compartment i as $\mathcal{V}_i^-(x)$ and the rate of transfer of individuals into compartment i by all other means as $\mathcal{V}_i^+(x)$. Thus, our system can be expressed in a condensed version as $\dot{\mathbf{x}}_i = \mathcal{F}_i(x) - \mathcal{V}_i(x)$ where $\mathcal{V}_i(x) = \mathcal{V}_i^-(x) - \mathcal{V}_i^+(x)$ for $i = 1, \ldots, 8$.

Next, we compute $\mathbf{F} = [\frac{\partial \mathcal{F}_i}{\partial x_j}(\mathbf{x}_0)]$ and $\mathbf{V} = [\frac{\partial \mathcal{V}_i}{\partial x_j}(\mathbf{x}_0)]$ for the exposed and infected compartments, namely for $1 \le i, j \le 5$, where $\mathbf{x}_0 = [0, 0, 0, 0, 0, N_h, 0, N_v]$ is the disease free equilibrium state with N_h and N_v being the initial population sizes of humans and mosquitoes respectively, and obtain the following 5×5 matrices:

$$\mathbf{F} = \begin{pmatrix} 0 & 0 & 0 & 0 & \beta_{hv}\sigma_v \\ 0 & 0 & 0 & 0 & 0 \\ 0 & 0 & 0 & 0 & 0 \\ 0 & \frac{\beta_{vh}\sigma_v N_v}{N_h} & \frac{\beta_{vh}\sigma_v N_v}{N_h} & 0 & 0 \\ 0 & 0 & 0 & 0 & 0 \end{pmatrix},$$

$$\mathbf{V} = \begin{pmatrix} \nu_h & 0 & 0 & 0 & 0 \\ -\nu_h\psi & \gamma_h & 0 & 0 & 0 \\ -\nu_h(1-\psi) & 0 & \gamma_h & 0 & 0 \\ 0 & 0 & 0 & \mu_v + \nu_v & 0 \\ 0 & 0 & 0 & -\nu_v & \mu_v \end{pmatrix}$$

Hence, we calculate the reproductive number as:

$$\mathcal{R}_0 := \rho(FV^{-1}) = \frac{\sigma_v \sqrt{N_v \beta_{hv} \beta_{vh} \nu_v}}{\sqrt{N_h \gamma_h \mu_v (\mu_v + \nu_v)}} = \sqrt{R_{hv} R_{vh}}$$

where $\rho(A)$ represents the spectral radius of the matrix A, and we have defined the quantities $R_{hv} = \left(\frac{\nu_v}{\mu_v+\nu_v}\right)\left(\frac{\sigma_v}{\mu_v}\right)\beta_{hv}$ and $R_{vh} = \left(\frac{N_v}{N_h}\right)\left(\frac{\sigma_v}{\gamma_h}\right)\beta_{vh}$.

Here, R_{hv} is the expected number of secondary infections in a fully susceptible human population resulting from one newly introduced infected mosquito. It is composed of the product of three terms. The first term, $\frac{\nu_v}{\mu_v+\nu_v}$, represents the probability that an exposed mosquito will survive the extrinsic incubation period. The second term, $\frac{\sigma_v}{\mu_v}$, is the number of human bites an infectious mosquito would make if humans were freely available. The third term, β_{hv}, is the probability of transmission occurrence given that a human is bitten by an infected mosquito. The number of secondary infections in a fully susceptible population of mosquitoes resulting from one newly introduced infected human is represented by R_{vh}. This value is also formed by the product of three terms. The first, $\frac{N_v}{N_h}$, is the vector to host ratio. The $\frac{\sigma_v}{\gamma_h}$ term is the maximum number of bites an infectious human will experience before recovery without impediment to mosquito bites. Finally, given that a susceptible mosquito bites an infectious human, β_{vh} is the probability of transmission from human to mosquito. The type reproductive number, or expected number of secondary human cases resulting from one newly infectious human, is ${\mathcal{R}_0}^T := (\mathcal{R}_0)^2$ (Manore et al., 2014).

A.3 Data model formulation

To use Bayes Theorem and obtain the posterior distributions, we calculate the data model as follows:

$$\begin{aligned}
f(\mathrm{Y}|\boldsymbol{\Theta}) &= \prod_{i=1}^{\tau^*} \mathrm{P}(E^*_{i+h_i}|\boldsymbol{\Theta})\mathrm{P}(I^*_{i+h_i}|\boldsymbol{\Theta})\cdots\mathrm{P}(dIv^*_{i+h_i}|\boldsymbol{\Theta}) \\
&= \prod_{i=1}^{\tau^*} \mathrm{Bin}(S_i, 1-\exp(-\lambda_h h_i))\mathrm{Bin}(E_i, 1-\exp(-\nu_h h_i))\cdots\mathrm{Bin}(Iv_i, 1-\exp(-\mu_h h_i)) \\
&= \prod_{i=1}^{\tau^*} \frac{S_i!}{(S_i - E^*_{i+h_i})!(E^*_{i+h_i}!)(1-\exp(-\nu_h h_i)))}^{E^*_{i+h_i}} \exp(-\nu_h h_i)^{S_i - E^*_{i+h_i}} \cdots \\
&\quad \prod_{i=1}^{\tau^*} \frac{Iv_i!}{(Iv_i - dIv^*_{i+h_i})!(dIv^*_{i+h_i}!)(1-\exp(-\mu_h h_i)))}^{dIv^*_{i+h_i}} \exp(-\mu_h h_i)^{Iv_i - dIv^*_{i+h_i}}.
\end{aligned}$$

A.4 Other parameter distributions

See Figs. 14 and 15, and Tables 11 and 12.

A.5 Other reproductive number distributions

See Fig. 16 and Table 13.

References

Andraud, M., Hens, N., Marais, C., Beutels, P., 2012. Dynamic epidemiological models for dengue transmission: a systematic review of structural approaches. PLoS One 7 (11), e49085.

Boorman, J., Porterfield, J., 1956. A simple technique for infection of mosquitoes with viruses transmission of Zika virus. Trans. R. Soc. Trop. Med. Hyg. 50 (3), 238–242.

Campos, G.S., Bandeira, A.C., Sardi, S.I., 2015. Zika virus outbreak, Bahia, Brazil. Emerg. Infect. Dis. 21 (10), 1885.

Cardoso, C.W., Paploski, I.A., Kikuti, M., Rodrigues, M.S., Silva, M.M., Campos, G.S., Sardi, S.I., Kitron, U., Reis, M.G., Ribeiro, G.S., 2015. Outbreak of exanthematous illness associated with Zika, chikungunya, and dengue viruses, Salvador, Brazil. Emerg. Infect. Dis. 12 (12), 2274.

Cauchemez, S., Besnard, M., Bompard, P., Dub, T., Guillemette-Artur, P., Eyrolle-Guignot, D., Salje, H., Van Kerkhove, M.D., Abadie, V., Garel, C., et al., 2016. Association between Zika virus and microcephaly in French Polynesia, 2013–15: a retrospective study. Lancet 387 (10033), 2125–2132.

Center for Disease Control, 2016a. Zika Transmission and Risk (accessed 30.10.16).

Center for Disease Control, 2016b. Zika Virus (accessed 21.01.17).

Chapman, J.D., Evans, N.D., 2009. The structural identifiability of susceptible-infective-recovered type epidemic models with incomplete immunity and birth targeted vaccination. Biomed. Signal Process. Control 4 (4), 278–284.

Coelho, F.C., Durovni, B., Saraceni, V., Lemos, C., Codeco, C.T., Camargo, S., de Carvalho, L.M., Bastos, L., Arduini, D., Villela, D.A., et al., 2016. Higher incidence of Zika in adult women than adult men in Rio de Janeiro suggests a significant contribution of sexual transmission from men to women. Int. J. Infect. Dis. 51, 128–132.

Countrymeters, 2016. Country Meters World Population (accessed 22.06.16).

Delatte, H., Gimonneau, G., Triboire, A., Fontenille, D., 2009. Influence of temperature on immature development, survival, longevity, fecundity, and gonotrophic cycles of *Aedes albopictus*, vector of chikungunya and dengue in the Indian Ocean. J. Med. Entomol. 46 (1), 33–41.

Diekmann, O., Heesterbeek, J.A.P., Metz, J.A., 1990. On the definition and the computation of the basic reproduction ratio r_0 in models for infectious diseases in heterogeneous populations. J. Math. Biol. 28 (4), 365–382.

Dudley, D.M., Aliota, M.T., Mohr, E.L., Weiler, A.M., Lehrer-Brey, G., Weisgrau, K.L., Mohns, M.S., Breitbach, M.E., Rasheed, M.N., Newman, C.M., et al., 2016. A rhesus macaque model of Asian-lineage Zika virus infection. Nat. Commun. 7.

Duffy, M.R., Chen, T.-H., Hancock, W.T., Powers, A.M., Kool, J.L., Lanciotti, R.S., Pretrick, M., Marfel, M., Holzbauer, S., Dubray, C., et al., 2009. Zika virus outbreak on yap island, federated states of Micronesia. N. Engl. J. Med. 360 (24), 2536–2543.

Eisenberg, M.C., Robertson, S.L., Tien, J.H., 2013. Identifiability and estimation of multiple transmission pathways in cholera and waterborne disease. J. Theor. Biol. 324, 84–102.

Elderd, B.D., Dukic, V.M., Dwyer, G., 2006. Uncertainty in predictions of disease spread and public health responses to bioterrorism and emerging diseases. Proc. Natl. Acad. Sci. 103 (42), 15693–15697.

Evans, N.D., White, L.J., Chapman, M.J., Godfrey, K.R., Chappell, M.J., 2005. The structural identifiability of the susceptible infected recovered model with seasonal forcing. Math. Biosci. 194 (2), 175–197.

Fay, R.W., 1964. The biology and bionomics of *Aedes aegypti* in the laboratory. Mosq. News 24 (3), 300–308.

Fonseca, K., Meatherall, B., Zarra, D., Drebot, M., MacDonald, J., Pabbaraju, K., Wong, S., Webster, P., Lindsay, R., Tellier, R., 2014. First case of Zika virus infection in a returning Canadian traveler. Am. J. Trop. Med. Hyg. 91 (5), 1035–1038.

Foy, B.D., Kobylinski, K.C., Chilson Foy, J.L., Blitvich, B.J., Travassos da Rosa, A., Haddow, A.D., Lanciotti, R.S., Tesh, R.B., 2011. Probable non-vector-borne transmission of Zika virus, Colorado, USA. Emerg. Infect. Dis. 17 (5), 880–882.

Funk, S., Kucharski, A.J., Camacho, A., Eggo, R.M., Yakob, L., Murray, L.M., Edmunds, W.J., 2016. Comparative analysis of dengue and Zika outbreaks reveals differences by setting and virus. PLoS Neg1. Trop. Dis. 10 (12), e0005173.

Gao, D., Lou, Y., He, D., Porco, T.C., Kuang, Y., Chowell, G., Ruan, S., 2016. Prevention and Control of Zika Fever as a Mosquito-borne and Sexually Transmitted Disease, arXiv preprint arXiv:1604.04008.

Hethcote, H.W., 2000. The mathematics of infectious diseases. SIAM Rev. 42 (4), 599–653.

Hyer, R., Covello, V., 2017. Top Questions on Zika: Simple Answers (accessed 23.05.17).

King, A.A., de Cellès, M.D., Magpantay, F.M., Rohani, P., 2015. Avoidable errors in the modelling of outbreaks of emerging pathogens, with special reference to ebola. Proc. R. Soc. B 282 (1806), The Royal Society, p. 20150347.

Kucharski, A.J., Funk, S., Eggo, R.M., Mallet, H.-P., Edmunds, W.J., Nilles, E.J., 2016. Transmission dynamics of Zika virus in island populations: a modelling analysis of the 2013–14 French Polynesia outbreak. PLoS Negl. Trop. Dis. 10 (5), e0004726.

Lekone, P.E., Finkenstädt, B.F., 2006. Statistical inference in a stochastic epidemic Seir model with control intervention: ebola as a case study. Biometrics 62 (4), 1170–1177.

Lessler, J., Ott, C.T., Carcelen, A.C., Konikoff, J.M., Williamson, J., Bi, Q., Reich, N.G., Cummings, D.A., Kucirka, L.M., Chaisson, L.H., 2016. Times to key events in the course of Zika infection and their implications for surveillance: a systematic review and pooled analysis. bioRxiv, 041913.

Lozano-Fuentes, S., Hayden, M.H., Welsh-Rodriguez, C., Ochoa-Martinez, C., Tapia-Santos, B., Kobylinski, K.C., Uejio, C.K., Zielinski-Gutierrez, E., Delle Monache, L., Monaghan, A.J., et al., 2012. The dengue virus mosquito vector

Aedes aegypti at high elevation in Mexico. Am. J. Trop. Med. Hyg. 87 (5), 902–909.
Manore, C.A., Hickmann, K.S., Xu, S., Wearing, H.J., Hyman, J.M., 2014. Comparing dengue and chikungunya emergence and endemic transmission in *A. aegypti* and *A. albopictus*. J. Theor. Biol. 356, 174–191.
Manore, C., Ostfeld, R., Agusto, F., Gaff, H., LaDeau, S., 2016. Defining the risk of Zika and chikungunya virus transmission in human population centers of the eastern United States. bioRxiv, 061382.
Mode, C.J., Sleeman, C.K., 2000. Stochastic Processes in Epidemiology: HIV/AIDS, Other Infectious Diseases and Computers. World Scientific.
Moreno, V., Espinoza, B., Bichara, D., Holechek, S.A., Castillo-Chavez, C., 2016. Role of Short-term Dispersal on the Dynamics of Zika Virus, arXiv preprint arXiv:1603.00442.
Nishiura, H., Kinoshita, R., Mizumoto, K., Yasuda, Y., Nah, K., 2016. Transmission potential of Zika virus infection in the south pacific. Int. J. Infect. Dis. 45, 95–97.
Ortenzio, D., Matheron, E., de Lamballerie, S., Hubert, X., Piorkowski, B., Maquart, G., Descamps, M., Damond, D., Yazdanpanah, F.Y., Leparc-Goffart, I., 2016. Evidence of sexual transmission of Zika virus. N. Engl. J. Med. 374 (22), 2195–2198.
Otero, M., Solari, H.G., Schweigmann, N., 2006. A stochastic population dynamics model for *Aedes aegypti*: formulation and application to a city with temperate climate. Bull. Math. Biol. 68 (8), 1945–1974.
Pan American Health Organization, 2016a. Number of Reported Cases of Dengue and Severe Dengue (DS) in the Americas, by Country (accessed 22.06.17).
Pan American Health Organization, 2016b. Cumulative Zika Suspected and Confirmed Cases Reported by Countries and Territories in the Americas-Interactive Epicurves (accessed 22.06.16).
Pan American Health Organization, 2017. Zika Cases and Congenital Syndrome Associated with Zika Virus Reported by Countries and Territories in the Americas, 2015–2017 Cumulative Cases Data as of 5 January 2017 2:00 PM EST (accessed 10.01.17).
Perkins, T.A., Siraj, A.S., Ruktanonchai, C.W., Kraemer, M.U., Tatem, A.J., 2016. Model-based projections of Zika virus infections in childbearing women in the Americas. Nat. Microbiol. 1, 16126.
Petersen, E., Staples, J., Meaney-Delman, D., et al., 2016. Interim guidelines for pregnant women during a Zika virus outbreak? United States, 2016. Morb. Mortal. Wkly. Rep. 2016 (65), 30–33.
Porter, A.T., Oleson, J.J., 2013. A path-specific seir model for use with general latent and infectious time distributions. Biometrics 69 (1), 101–108.
Porter, A.T., Oleson, J.J., 2016. A spatial epidemic model for disease spread over a heterogeneous spatial support. Stat. Med. 35 (5), 721–733.
Rojas, D.P., Dean, N.E., Yang, Y., Kenah, E., Quintero, J., Tomasi, S., Ramirez, E.L., Kelly, Y., Castro, C., Carrasquilla, G., et al., 2016. The epidemiology and transmissibility of Zika virus in Girardot and San Andres Island, Colombia, September 2015 to January 2016. Euro Surveill. 21 (28).
Rubin, D.B., et al., 1984. Bayesianly justifiable and relevant frequency calculations for the applied statistician. Ann. Stat. 12 (4), 1151–1172.
Sivanathan, M., (Ph.D. thesis) 2006. The ecology and biology of *Aedes aegypti* (L.) and *Aedes albopictus* (Skuse) (Diptera: Culicidae) and the resistance status of *Aedes albopictus* (field strain) against organophosphates in Penang, Malaysia [QL536.M266 2006 f rb]. Universiti Sains Malaysia.
Towers, S., Brauer, F., Castillo-Chavez, C., et al., 2016. Estimation of the reproduction number of the 2015 Zika virus outbreak in Barranquilla, Colombia, and a first estimate of the relative role of sexual transmission [internet]. arxiv.2016. Reference Source.
Van den Driessche, P., Watmough, J., 2002. Reproduction numbers and sub-threshold endemic equilibria for compartmental models of disease transmission. Math. Biosci. 180 (1), 29–48.
Venturi, G., Zammarchi, L., Fortuna, C., Remoli, M., Benedetti, E., Fiorentini, C., Trotta, M., Rizzo, C., Mantella, A., Rezza, G., et al., 2016. An autochthonous case of Zika due to possible sexual transmission, Florence, Italy, 2014. Euro Surveill. 21 (8), 30148.
Villela, D., Bastos, L., de Carvalho, L., Cruz, O., Gomes, M., Durovni, B., Lemos, M., Saraceni, V., Coelho, F., Codeço, C., 2017. Zika in Rio de Janeiro: assessment of basic reproduction number and comparison with dengue outbreaks. Epidemiol. Infect., 1–9.
Wong, P.-S.J., Li, M.-z.I., Chong, C.-S., Ng, L.-C., Tan, C.-H., 2013. *Aedes* (Stegomyia) *albopictus* (Skuse): a potential vector of Zika virus in Singapore. PLoS Negl. Trop. Dis. 7 (8), e2348.
World Health Organization, 2016. Western Pacific Region. Zika Virus Fact Sheet (accessed 22.03.16).
World Health Organization, 2017a. The History of Zika virus (accessed 21.01.17).
World Health Organization, 2017b. One Year Into the Zika Outbreak: How an Obscure Disease Became a Global Health Emergency (accessed 23.05.17).